

**NASA CONTRACTOR
REPORT**



NASA CR-1027

NASA CR-1027

GPO PRICE \$ _____

CFSTI PRICE(S) \$ _____

Hard copy (HC) _____

Microfiche (MF) _____

ff 653 July 65

FA-111111 FORM 602

(ACCESSION NUMBER)

(THRU)

(PAGES)

(CODE)

NUMBER OF THIS REPORT

CATEGORY

INVISCID FLOW FIELD INDUCED BY A ROTOR IN GROUND EFFECT

by Michael D. Greenberg and Alvin L. Kaskel

Prepared by

THERM ADVANCED RESEARCH, INC.

Ithaca, N. Y.

for Langley Research Center

INVISCID FLOW FIELD
INDUCED BY A ROTOR IN GROUND EFFECT

By Michael D. Greenberg and Alvin L. Kaskel

Distribution of this report is provided in the interest of information exchange. Responsibility for the contents resides in the author or organization that prepared it.

Prepared under Contract No. NAS 1-6349 by
THERM ADVANCED RESEARCH, INC.
Ithaca, N.Y.

for Langley Research Center

NATIONAL AERONAUTICS AND SPACE ADMINISTRATION

INVISCID FLOW FIELD
INDUCED BY A ROTOR IN GROUND EFFECT

By Michael D. Greenberg and Alvin L. Kaskel
Therm Advanced Research, Inc.

SUMMARY

The inviscid flow field induced by a rotor in ground effect is calculated based upon an actuator disk model of the rotor, for the case of a constant circulation distribution over the blade radius. The governing nonlinear integral equations are solved by a systematic iterative scheme which is similar to the Newton-Raphson method for the solution of nonlinear algebraic equations. Numerical results are presented for both the ground-effect case and the out-of-ground-effect limit.

INTRODUCTION

Several important problems arise in connection with a rotor hovering in ground effect, such as downwash impingement, and the effect of rotor-ground interference on the blade loading.

In the present paper, we are concerned with the problem of downwash impingement. Of the various aspects of this problem, we will confine our attention to the calculation of the inviscid flow field. This is of special importance since it is required as input for the subsequent calculation of the ground boundary layer and particle entrainment.

A numerical investigation of the inviscid flow field induced by a finite-bladed rotor has been carried out at the Cornell Aeronautical Laboratory, over the past several years, by W. G. Brady, P. Crimi, F. A. DuWaldt, and A. Sowyrd. Initially, they represented the rotor wake by discrete (finite core) vortex rings released periodically from the edge of the rotor disk (References 1,2). More recently, they have used a wake model based upon distorted continuous helices emanating from the blade tips (Reference 3).

In contrast, we will consider the axisymmetric flow field associated with an actuator disk representation of the rotor. The governing nonlinear integral equations will be solved by a systematic iterative procedure which is based upon the Newton-Raphson method for the solution of nonlinear algebraic equations (Reference 4). The mathematical treatment is somewhat general and could, we believe, be applied to other nonlinear free-boundary problems.

The nonlinear actuator disk, in the absence of ground effect, has already been treated in an important paper by T. Y. Wu (Reference 5), although numerical

results are not yet available. The work of H. R. Chaplin (Reference 6) should also be noted, even though it deals with the shrouded disk, since that problem is fundamentally similar to the one treated here. Both Wu and Chaplin employ iterative schemes which differ appreciably from the one developed in the present paper.

The authors would like to thank their colleagues, Messrs. J. C. Erickson, Jr. and G. R. Hough, for many helpful discussions during the course of this work.

PRINCIPAL NOMENCLATURE

a_j	coefficients in expansion of slipstream vorticity
b_j	coefficients in expansion of slipstream radius
C	loading coefficient
C_T	thrust coefficient, $\text{thrust}/\bar{\rho}(\Omega R)^2(\pi R^2)$
f_j	matching functions for slipstream shape
F	function in dynamic equation, $C - C^2/4T^2(x)$
F_∞	F with $T(x)$ replaced by T_∞
g_j	matching functions for slipstream vorticity
G	Green's function for L , over the infinite domain $-\infty < x < \infty$, $r < \infty$
h_j	modified f_j 's for ground-effect case
L	linear differential operator, $\nabla^2 - r^{-2}$
M	number of shape collocation points
n	iteration index
N	number of gamma collocation points
p	static pressure
q	fluid velocity, $(u^2 + v^2 + w^2)^{1/2}$
$Q_{\pm 1/2}$	Legendre functions of second kind and degree $\pm 1/2$
t, T	slipstream radius, with arguments ξ and x respectively
u, v, w	x, r, θ fluid velocity components
U	free-stream speed

x, r, θ	cylindrical coordinates
X	x-location of ground plane
α, β	damping factors
γ, γ_s	slipstream circulation per unit x-length and arc-length, respectively
γ_∞	asymptotic value of γ
Γ	blade circulation distribution
ζ	meridional velocity, $(u^2 + v^2)^{\frac{1}{2}}$
λ	advance ratio, $U/\Omega R$
ξ, ρ	dummy x, r variables, respectively
$\tilde{\rho}$	fluid mass density
Ψ	stream function
Ψ_∞	value of Ψ on the slipstream
$\tilde{\omega}_{1,2}$	Legendre function arguments
Ω	blade rotational velocity, radians per unit time
$()'$	prime denotes perturbational quantity
$()_x$	subscripted variable denotes partial differentiation with respect to that variable
$()^{(n)}$	n th iterate
$\sqrt{\quad}$	$d(\text{arc-length})/dx$, $[1 + (dT/dx)^2]^{\frac{1}{2}}$

NOTE: Prior to equation (21), all quantities are in dimensional form. Starting with equation (21), they are nondimensionalized as follows: lengths with respect to R ; velocities, γ and γ_s with respect to ΩR ; Γ with respect to ΩR^2 ; and Ψ with respect to ΩR^3 . However, for notational simplicity we omit any explicit reminder of nondimensionalization, such as primes or asterisks.

THEORETICAL DEVELOPMENT

Out-of-Ground-Effect Limit; Actuator Disk Theory

Governing Nonlinear Differential Equation. Let us consider a propeller of blade radius R and negligible hub radius, operating relative to a uniform free stream U . We consider the blade number to be infinite, the so-called "actuator disk" model, and view the steady axisymmetric flow from a Newtonian x, r, θ coordinate system; see Fig. 1 (where we have sketched only one of the infinitely

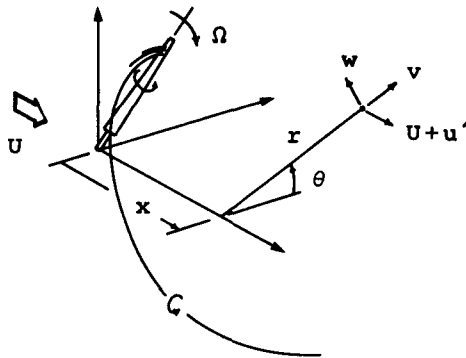


Figure 1. Coordinates and Geometry

many blades). The static actuator disk, i.e. for $U=0$, is equivalent to our hovering rotor out of ground effect. We will, however, retain an arbitrary U in our analysis since it presents no additional difficulty and, at the same time, extends the applicability of our solution from the static condition, up to the light loading limit (where $U \gg$ the perturbational velocities).

The flow field is defined by the x, r, θ velocity components u, v, w respectively, or - equivalently - by w and a stream function Ψ , such that

$$u = U + u' = \Psi_r / r \tag{1}$$

$$v = v' = -\Psi_x / r \tag{2}$$

where the primed terms are perturbational quantities, and subscripts denote partial differentiation.

It has been shown by Wu (Reference 4), that Ψ must satisfy the following nonlinear partial differential equation,

$$\Psi_{rr} - r^{-1}\Psi_r + \Psi_{xx} = - (\Omega r^2 + wr) d(wr)/d\Psi \quad (3)$$

Briefly, this may be derived by computing the circulation about an elemental meridional area $dxdr$, in two different ways: According to Stokes' theorem it may be computed as the θ component of vorticity, $v_x - u_r$, times the area $dxdr$, or, alternatively, as the line integral of " $\underline{q} \cdot d\underline{r}$ " around the circumference of the element. Equating these two results produces (3).

Conversion to an Integral Equation. It will be convenient to convert (3) to an integral equation. With $L \equiv \nabla^2 - r^{-2}$ and $\Psi = Ur^2/2 + \Psi'$, we can express (3) in the form

$$L(\Psi'/r) = - (\Omega r + w) d(wr)/d\Psi \quad (4)$$

Noting that L is linear (the nonlinearity being confined to the right hand side) we apply the method of Green's functions: Specifically, we seek the Green's function G as the solution of the associated equation

$$L(G/r) = -\delta(x-\xi)\delta(r-\rho) \quad (5)$$

with the δ 's denoting Dirac delta functions. Multiplying (5) through by $rJ_1(\bar{r}r)\exp(-i\bar{x}x)$ and integrating on r from $0 \rightarrow \infty$ and on x from $-\infty \rightarrow \infty$, we obtain

$$\rho J_1(\bar{r}\rho) e^{-i\bar{x}\xi} / (\bar{x}^2 + \bar{r}^2) \quad (6)$$

as the Hankel-Fourier transform of G/r , where J_1 denotes the Bessel function of the first kind and order one. Carrying out the Fourier inversion using the calculus of residues, and the Hankel inversion with the help of formula (2) on page 389 of Reference 7, we obtain

$$G(\xi, \rho; x, r) = r^{\frac{1}{2}} \rho^{\frac{1}{2}} Q_{\frac{1}{2}}(\tilde{\omega}) / 2\pi \quad (7)$$

where $Q_{\frac{1}{2}}$ is the Legendre function of second kind and degree $\frac{1}{2}$, with argument

$$\tilde{\omega} = 1 + [(\xi-x)^2 + (\rho-r)^2] / 2\rho r \quad (8)$$

This is equivalent to the forms given by Wu and Chaplin. Physically, we may identify G as the stream function induced at a field point x, r, θ by a ring

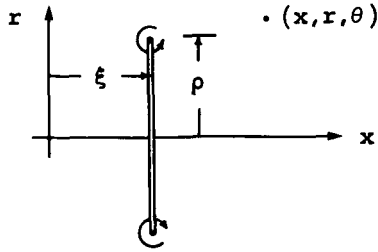


Figure 2. Interpretation of the Green's Function

vortex of unit strength, as shown in Fig. 2 .

With the Green's function in hand, we may re-express (3) in the form

$$\Psi(x,r) = Ur^2/2 + \iint_D \frac{r^{1/2} \rho^{1/2}}{2\pi} Q_{1/2}(\tilde{\omega}) (\Omega\rho + w) \frac{d(w\rho)}{d\Psi} d\rho d\xi \quad (9)$$

This is a nonlinear integral equation in the two unknowns Ψ and D . The region D is clearly the slipstream, since w - and hence $d(w\rho)/d\Psi$ - is zero outside the slipstream, by application of Kelvin's theorem.

Reduction for Uniform Circulation Distribution. For the case of uniform blade circulation distribution we have

$$\begin{aligned} w\rho &= \text{constant} = -\Gamma/2\pi & , & \text{inside } D \\ &= 0 & , & \text{outside } D \end{aligned} \quad (10)$$

where Γ is the strength of the "hub" vortex, coinciding with the positive x axis. Converting the ρ, ξ integration variables to Ψ, ξ according to $d\rho d\xi = d\Psi d\xi / (\partial\Psi/\partial\rho)$, the Ψ integration can be carried out explicitly since the $d(w\rho)/d\Psi$ term in the integrand is zero except at the hub and tip; $\rho = 0, R$. Of these two contributions, the hub portion is zero since $\rho^{1/2} Q_{1/2} = 0$ at $\rho = 0$. The resulting integral equation, then, is

$$\Psi(x,r) = Ur^2/2 + \frac{r^{1/2}}{4\pi^2} \int_0^\infty \left\{ \Omega\Gamma t^{3/2} - \frac{\Gamma^2}{4\pi} t^{-1/2} \right\} Q_{1/2}(\tilde{\omega}_1) \frac{d\xi}{\partial\Psi/\partial\rho} \Big|_{\rho=t} \quad (11)$$

where $t(\xi)$ will denote the slipstream radius, and $\tilde{\omega}_1$ is identical to $\tilde{\omega}$, with ρ replaced by $t(\xi)$.

Vortex Sheet Interpretation. Although we can work directly with (11), we prefer to re-express the integral term in terms of an equivalent vortex representation of the slipstream; specifically, a distribution of ring vortices*, of circulation $\gamma(\xi)$ per unit ξ -length, over the slipstream surface $\rho = t(\xi)$.

According to our physical interpretation of the Green's function G , we can therefore express $\Psi(x,r)$ in the form

$$\Psi(x,r) = Ur^2/2 + \int_0^\infty G(\xi,t;x,r) \gamma(\xi) d\xi \quad (12)$$

We can establish the equivalence between (11) and (12) as follows:

Applying the Bernoulli equation to streamline A (see Fig. 3) between the points " ∞ " and (ξ, t^+) , we have

$$P_A + \frac{1}{2} \tilde{\rho} q_A^2 = P_\infty + \frac{1}{2} \tilde{\rho} U^2 \quad (13)$$

where $\tilde{\rho}$ is the fluid mass density and $q^2 \equiv u^2 + v^2 + w^2$.

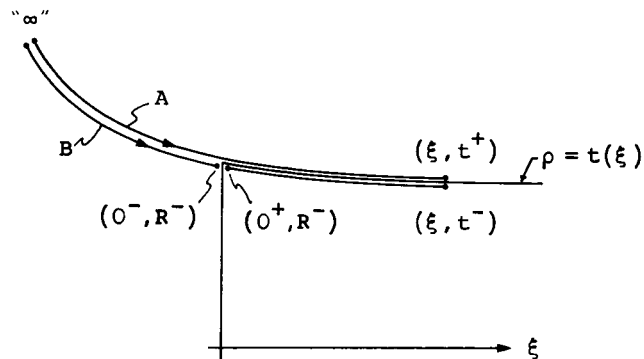


Figure 3. Application of Bernoulli Equation

* There will also be a distribution of vortices, over the slipstream surface, which are oriented axially. These contribute to w but not to Ψ , and will not directly concern us.

If we also apply it to streamline B, from " ∞ " to $(0^-, R^-)$ and then from $(0^+, R^-)$ to (ξ, t^-) , we find that

$$p_B + \frac{1}{2}\tilde{\rho}q_B^2 = p_\infty + \frac{1}{2}\tilde{\rho}U^2 + \frac{1}{2}\tilde{\rho}w^2(0^+, R^-) + \Delta p \quad (14)$$

where Δp is the pressure jump across the propeller plane at $\rho = R^-$. Now, the slipstream vorticity drifts freely so that we must have $p_B - p_A = 0$. Subtracting (13) from (14), then,

$$0 = p_B - p_A = \Delta p - \frac{1}{2}\tilde{\rho}(q_B^2 - q_A^2) + \frac{1}{2}\tilde{\rho}w^2(0^+, R^-) \quad (15)$$

The first and last terms on the right side are simply

$$\begin{aligned} \Delta p &= d(\text{thrust})/2\pi\rho d\rho \\ &= \tilde{\rho}(\Omega\rho - \Gamma/4\pi\rho)\Gamma d\rho/2\pi\rho d\rho \end{aligned} \quad (16)$$

at $\rho = R^-$, according to the Kutta-Joukowski formula, and

$$\frac{1}{2}\tilde{\rho}w^2(0^+, R^-) = \frac{1}{2}\tilde{\rho}(\Gamma/2\pi R)^2 \quad (17)$$

according to (10). To evaluate the middle term in (15), we note that

$$\begin{aligned} q_B^2 - q_A^2 &= (u^2 + v^2 + w^2)_B - (u^2 + v^2 + w^2)_A \\ &= \zeta_B^2 - \zeta_A^2 + \Gamma^2/4\pi^2 t^2 \end{aligned} \quad (18)$$

where we have defined the "meridional" velocity, $\zeta \equiv (u^2 + v^2)^{1/2}$, and have used the fact that $w_B = \Gamma/2\pi t$ and $w_A = 0$ from (10). Finally,

$$\begin{aligned} \zeta_B^2 - \zeta_A^2 &= (\zeta_B - \zeta_A)(\zeta_B + \zeta_A) \\ &= (\gamma_s)(2\zeta) = 2\gamma u \end{aligned} \quad (19)$$

where γ_s denotes the slipstream circulation per unit arc-length along the slipstream. Combining (15)-(19), we may express the force-free condition on

the slipstream in the simple form

$$\gamma u = \frac{\Omega \Gamma}{2\pi} - \frac{\Gamma^2}{8\pi^2 t^2} \quad (20)$$

If we solve (20) for γ , noting that $u = \Psi_\rho / \rho$ at $\rho = t$, we find that the integral term in (12) is, in fact, identical to the one in (11), thus establishing the validity of our vortex sheet representation.

The Final Integral Equations. First, let us non-dimensionalize as follows: lengths with respect to R ; velocities, γ and γ_s with respect to ΩR ; Γ with respect to ΩR^2 ; and Ψ with respect to ΩR^3 . For notational simplicity we will omit any explicit reminder of nondimensionalization, such as asterisks or primes, in the remainder of the report. Equations (12) and (20), for example, may therefore be rewritten as

$$\Psi(x, r) = \lambda r^2/2 + \int_0^\infty G(\xi; t; x, r) \gamma(\xi) d\xi \quad (21)$$

$$\gamma u = \frac{c}{2} - \frac{c^2}{8t^2} \quad (22)$$

respectively, where we have defined an advance ratio $\lambda \equiv U/\Omega R$, and a "loading coefficient" $c \equiv \Gamma/\pi$.

Whereas the integral equation (21) contains both the kinematics and dynamics, we prefer to express these conditions separately. The kinematic condition on the slipstream is that it be a streamline (more precisely, an axisymmetric stream surface). Setting $r = T(x)^*$ in (21), we have

$$\Psi_\infty = \lambda T^2/2 + \int_0^\infty G(\xi, t; x, T) \gamma d\xi \quad (23)$$

where we have set $\Psi(0, 1) = \Psi[\infty, T(\infty)] \equiv \Psi(\infty, T_\infty) \equiv \Psi_\infty$.

The dynamic condition is given by (22). Changing the independent variable from ξ to x , and noting that $u = \Psi_x/r$ at $r = T$, with Ψ_x obtained from (21), we obtain

* It will be convenient to express the slipstream radius as t or T depending on whether the argument is the integration variable ξ or the field point x , respectively.

$$\left\{ \frac{c}{2} - \frac{c^2}{8T^2} \right\} \frac{T}{\gamma} - \lambda T = \int_0^{\infty} G_T(\xi, t; x, T) \gamma \, d\xi \quad (24)$$

Equations (23) and (24), then, constitute two coupled nonlinear integral equations in the two unknowns γ and T , and are to be satisfied over the extent of the slipstream, $0 < x < \infty$.

The kernels are as follows:

$$\begin{aligned} G &= T^{\frac{1}{2}} t^{\frac{1}{2}} Q_{\frac{1}{2}}(\tilde{\omega}_2) / 2\pi \\ &= O(\ln|\xi-x|) \quad \text{as } \xi \rightarrow x \\ &= O(\xi^{-3}) \quad \text{as } \xi \rightarrow \infty \end{aligned} \quad (25)$$

where $\tilde{\omega}_2$ is identical to $\tilde{\omega}$, with ρ and r replaced by t and T respectively. Using the relation,

$$dQ_{\frac{1}{2}}(z)/dz = [zQ_{\frac{1}{2}}(z) - Q_{-\frac{1}{2}}(z)] / 2(z^2-1) \quad (26)$$

we may express

$$\begin{aligned} G_T &= [AQ_{\frac{1}{2}}(\tilde{\omega}_2) + BQ_{-\frac{1}{2}}(\tilde{\omega}_2)] / (\tilde{\omega}_2^2-1) \\ &= O(\xi-x)^{-1} \quad \text{as } \xi \rightarrow x \\ &= O(\xi^{-3}) \quad \text{as } \xi \rightarrow \infty \end{aligned} \quad (27)$$

where

$$\begin{aligned} A &= [T^2 - t^2 + (\xi-x)^2] / 8\pi T^{\frac{1}{2}} t^{\frac{3}{2}} \\ B &= [t^2 - T^2 + (\xi-x)^2] / 8\pi T^{\frac{3}{2}} t^{\frac{1}{2}} \end{aligned} \quad (28)$$

Finally, we point out that the integral in (24) is to be interpreted in the Cauchy principal value sense.

Asymptotic Behavior of the Unknowns. Before proceeding with the detailed solution of (23) and (24) let us examine the equations at $x=0$ and ∞ .

As $x \rightarrow \infty$, it is known that $T(x) \sim \text{constant} \equiv T_{\infty}$, say, and $\gamma(x) \sim \text{constant} \equiv \gamma_{\infty}$. With these quantities constant at $x=\infty$, the integrals in (23) and (24) can be evaluated analytically. Instead of pursuing the details

of the integration, let us use the known fact (e.g. Reference 8) that an infinite solenoid of constant radius and constant vortex strength, T_∞ and γ_∞ in our case, induces a velocity field given by

$$\begin{aligned} (u', v', w') &= (0, 0, 0) & , & \quad r > T_\infty \\ &= (\gamma_\infty/2, 0, 0) & , & \quad r = T_\infty \\ &= (\gamma_\infty, 0, 0) & , & \quad r < T_\infty \end{aligned} \quad (29)$$

Now, since $2\pi\Psi(\xi, \rho)$ is the mass flow through the disk $r < \rho$ at $x = \xi$, we see - by virtue of (29) - that (23) must reduce to

$$\Psi_\infty = (\pi T_\infty^2)(\lambda + \gamma_\infty)/2\pi = T_\infty^2(\lambda + \gamma_\infty)/2 \quad (30)$$

at $x = \infty$. Noting that (24) is merely a re-statement of (22), we see also that (24) must reduce to

$$\gamma_\infty \left\{ \lambda + \frac{\gamma_\infty}{2} \right\} = \frac{C}{2} - \frac{C^2}{8T_\infty^2} \equiv \frac{F_\infty}{2} \quad (31)$$

at $x = \infty$, where we have introduced the quantity $F(x) \equiv C - C^2/4T^2(x)$ for convenience. Equation (31) can be solved for γ_∞ in the form

$$\gamma_\infty = (\lambda^2 + F_\infty)^{1/2} - \lambda \quad (32)$$

It is interesting to note that (30) and (32) constitute two equations in the three unknowns Ψ_∞ , T_∞ and γ_∞ so that the final slipstream contraction cannot be computed (in terms of the operating conditions λ and C) simply by investigation of the asymptotic behavior, but must await the complete solution of the governing equations (23) and (24).

Now let us see what can be said about the behavior of the unknowns at the lip of the slipstream; i.e. as $x \rightarrow 0$ through positive values. Consider, first, the static case, where $\lambda = 0$. Anticipating a flow field as sketched in Fig. 4, it is clear that the flow around the lip implies a square-root singularity in the circulation, so that $\gamma_s(x) = O(x^{-1/2})$ as $x \rightarrow 0$. This singularity should be present even when $\lambda > 0$, and will vanish only in the light loading limit where the slipstream-induced jet velocity is negligible compared to the free stream.

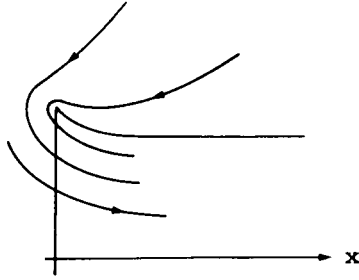


Figure 4. Flow Field for the Static Condition

Solution Based Upon the Newton-Raphson Method. With an exact solution of the highly nonlinear, coupled, integral equations (23) and (24) apparently out of the question, we will develop an iterative solution as follows. Starting with

$$T^{(0)}(x) = \text{constant} = 1 \quad (33)$$

$$\gamma^{(0)}(x) = \text{constant} = \gamma_{\infty}^{(0)} \quad (34)$$

we determine an improved slipstream shape, $T^{(1)}$, from (23); with $T=T^{(1)}$ we then determine an improved vortex distribution, $\gamma^{(1)}$, from (24); with $\gamma=\gamma^{(1)}$, $T^{(2)}$ is then computed from (23), and so on, until suitable convergence is attained. Our notation is to be interpreted in the obvious way. For example, $\gamma_{\infty}^{(0)}$ is given by (32) with F_{∞} replaced by $F_{\infty}^{(0)}$ which, in turn, is defined according to the same formula as $F(x)$ but with $T(x)$ replaced by $T_{\infty}^{(0)}$.

In order to carry out the solution of (23) for $T^{(n+1)}$ at each step we linearize all the terms in (23) about the previous iterate, $T^{(n)}$. Similarly, to solve (24) for $\gamma^{(n+1)}$ we expand the nonlinear term about $\gamma^{(n)}$. Specifically,

$$\begin{aligned} \psi_{\infty}^{(n+1)} &= T_{\infty}^{(n+1)2} (\lambda + \gamma_{\infty}^{(n)}) / 2 \\ &\approx [T_{\infty}^{(n)2} + 2T_{\infty}^{(n)} (T_{\infty}^{(n+1)} - T_{\infty}^{(n)})] (\lambda + \gamma_{\infty}^{(n)}) / 2 \end{aligned} \quad (35)$$

$$T^{(n+1)2} \approx T^{(n)2} + 2T^{(n)} (T^{(n+1)} - T^{(n)}) \quad (36)$$

$$G^{(n+1)} \approx G^{(n)} + G_T^{(n)} (T^{(n+1)} - T^{(n)}) + G_t^{(n)} (t^{(n+1)} - t^{(n)}) \quad (37)$$

in (23), where $G^{(n)}$ denotes $G(\xi, t^{(n)}; x, T^{(n)})$, and

$$1/\gamma^{(n+1)} \approx 1/\gamma^{(n)} - (1/\gamma^{(n)})^2 (\gamma^{(n+1)} - \gamma^{(n)}) \quad (38)$$

in (24). This "stepwise linearization" is, basically, analogous to the Newton-Raphson method for the solution of algebraic equations (Reference 4). We emphasize that (35)-(38) tend to equalities as the (presumably convergent) iteration proceeds, and therefore in no way compromise the full nonlinearity of (23) and (24).

Whereas the two "correction" terms in (38), for example, are supplied automatically by the mathematics, it is instructive to interpret them physically. Multiplying (23) through by 2π , for convenience, and taking $n=0$ for definiteness, the integral term is expanded, according to (38), in the form

$$\begin{aligned} 2\pi \int_0^\infty G^{(1)} \gamma^{(0)} d\xi &\approx 2\pi \int_0^\infty G^{(0)} \gamma^{(0)} d\xi + 2\pi \int_0^\infty G_T^{(0)} (T^{(1)} - T^{(0)}) \gamma^{(0)} d\xi \\ &+ 2\pi \int_0^\infty G_t^{(0)} (t^{(1)} - t^{(0)}) \gamma^{(0)} d\xi \equiv \textcircled{1} + \textcircled{2} + \textcircled{3} \quad (39) \end{aligned}$$

Now, $\textcircled{1}$ is easily identified as the mass flow rate induced through the disk AB (see Fig. 5) by $\gamma^{(0)}$ on $t^{(0)}$, whereas we really want the flow induced through AC by $\gamma^{(0)}$ on $t^{(1)}$ if (23) is to be an equality at that particular

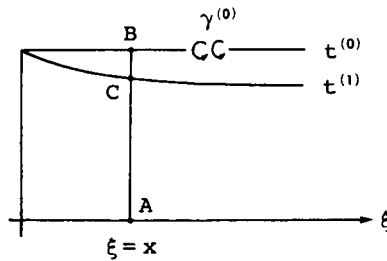


Figure 5. Interpretation of Correction Terms

value of x . The next term, $\textcircled{2}$, does in fact partially correct this by deducting (approximately) the flow through the annulus BC. To see this, let us re-express

$$\textcircled{2} = - \underbrace{2\pi T^{(0)} (T^{(0)} - T^{(1)})}_{(i)} \cdot \underbrace{\frac{1}{T^{(0)}} \int_0^{\infty} G_T^{(0)} \gamma^{(0)} d\xi}_{(ii)} \quad (40)$$

where (i) approximates the area of the annulus BC, and (ii) is the x-velocity induced at B by $\gamma^{(0)}$ on $t^{(0)}$.

The last term, $\textcircled{3}$, supplies an additional correction which is not, however, as easily interpreted in physical terms.

To provide a measure of control over the convergence of the iteration we introduce "damping factors" α and β so that the right hand side of (37) is replaced by

$$G^{(n)} + \alpha G_T^{(n)} (T^{(n+1)} - T^{(n)}) + \beta G_t^{(n)} (t^{(n+1)} - t^{(n)}) \quad (41)$$

Based upon numerical results, we have found that if $\alpha + \beta$ is too small, $T^{(n)}$ will be overcontracted and the iteration will diverge. An optimum is obtained, with regard to rapid convergence, when $\alpha + \beta$ is increased to approximately 1.8, independent of the disk loading. Curiously, the details of the iteration are quite insensitive as to how the "1.8" is divided between α and β . Consequently, we will take $\beta = 0$, from here on, for simplicity.

Actually, it is not surprising that with $\beta = 0$ the optimum $\alpha \approx 1.8$ since (ii) in (40) is the x-velocity computed right on the slipstream at B (Fig. 5) whereas the desired velocity just inside the slipstream is approximately twice as large*.

To proceed with the solution we expand

$$T^{(n)}(x) = 1 + \sum_{j=1}^M [f_j(x) - f_j(0)] b_j^{(n)} \quad (42)$$

$$\begin{aligned} \gamma^{(n)}(x) &= \sqrt{1 + (dT^{(n)}/dx)^2} \gamma_s^{(n)}(x) \\ &= \sqrt{\gamma^{(n)}} \gamma_{\infty}^{(n)} \left\{ 1 + \sum_{j=1}^N g_j(x) a_j^{(n)} \right\} \end{aligned} \quad (43)$$

* Recall from (29) that at $x = \infty$, u' inside the slipstream is exactly twice as large as it is on the slipstream. This is, in fact, a good approximation for finite x as well.

where the f_j 's and g_j 's are suitably chosen "matching functions" which tend to zero at infinity. The form of these expressions guarantees satisfaction of the required end conditions, $T^{(n)}(0) = 1$ and $\gamma^{(n)}(\infty) = \gamma_\infty^{(n)}$. In addition, at least one of the g_j 's include an $x^{-\frac{1}{2}}$ factor, to ensure the required square-root singularity at the lip.

Using the above expressions, our "kinematic" equation (23) can be re-written in the form

$$\int_0^\infty \left\{ -G^{(n)} + \alpha(T^{(n)} - 1)G_T^{(n)} \right\} \gamma^{(n)} d\xi + T_\infty^{(n)}(\lambda + \gamma_\infty^{(n)})(1 - T_\infty^{(n)}/2) - \lambda T^{(n)}(1 - T^{(n)}/2) = \sum_{j=1}^M \left\{ \alpha[f_j(x) - f_j(0)] \int_0^\infty G_T^{(n)} \gamma^{(n)} d\xi + \lambda T^{(n)}[f_j(x) - f_j(0)] + T_\infty^{(n)}(\lambda + \gamma_\infty^{(n)})f_j(0) \right\} b_j^{(n+1)} \quad (44)$$

and our "dynamic" equation (24) can be expressed as

$$\left\{ \frac{F^{(n+1)}(2\gamma_s^{(n)} - \gamma_\infty^{(n+1)})}{2\sqrt{\gamma^{(n+1)}}\gamma_s^{(n)2}} - \lambda \right\} \frac{T^{(n+1)}}{\gamma_\infty^{(n+1)}} - \int_0^\infty G_T^{(n+1)} \sqrt{\gamma^{(n+1)}} d\xi = \sum_{j=1}^N \left\{ \frac{F^{(n+1)}T^{(n+1)}g_j}{2\sqrt{\gamma^{(n+1)}}\gamma_s^{(n)2}} + \int_0^\infty G_T^{(n+1)} \sqrt{\gamma^{(n+1)}} g_j d\xi \right\} a_j^{(n+1)} \quad (45)$$

where it is understood that the " $\sqrt{\gamma}$ " terms are evaluated at ξ or x depending on whether they are under an integral sign or not, respectively; similarly for g_j , γ and γ_s .

Our solution proceeds as follows: Starting with $n=0$, we require the satisfaction of (44) at M "collocation" points x_1, \dots, x_M . This produces M simultaneous linear algebraic equations which are then solved for the unknown coefficients $b_1^{(1)}, \dots, b_M^{(1)}$. Next, we require the satisfaction of (45) at N collocation points (which need not coincide with the M points used to solve (44)) and hence compute $a_1^{(1)}, \dots, a_N^{(1)}$. The process is then repeated for $n = 1, 2, \dots$ until suitable convergence is attained.

We point out that instead of solving (23) and (24) successively for T and γ , we could have solved them simultaneously, at each step. Although this might lead to convergence in fewer iterations, the overall computing time would almost certainly be greater, however, since it takes approximately twice as long to generate an $(M+N)$ th order set of linear algebraic equations as it does to

generate M and N th order sets separately.

Interpretation of the Loading Coefficient. Before discussing our numerical results, let us clarify the physical significance of our "loading coefficient", $C = \Gamma/\pi$. Defining the thrust coefficient C_T as the thrust divided by $\tilde{\rho}(\Omega R)^2(\pi R^2)$, we may use the Kutta-Joukowski formula to express

$$C_T = \frac{1}{\pi} \int_0^1 \left\{ r - \frac{\Gamma(r)}{4\pi r} \right\} \Gamma(r) dr \quad (46)$$

Now, in our analysis we have considered the blade circulation distribution $\Gamma(r) = \text{constant} = \Gamma$ over $0 < r < 1$. For this case, the swirl term $(\Gamma/4\pi r)$ in the integrand causes the integral to diverge. In reality, however, $\Gamma(r)$ will drop to zero at a finite radius, say ϵ , where $0 < \epsilon < 1$. Replacing the lower integration limit by ϵ , the integration in (46) may be carried out, to give

$$C_T = C [1 - \epsilon^2 + (C/2) \ln \epsilon] / 2 \quad (47)$$

For typical values of C and ϵ , $\epsilon^2 - (C/2) \ln \epsilon$ is quite small compared to unity, so that the loading coefficient C is approximately twice the thrust coefficient C_T .

Numerical Results. As an illustration, let us consider the static case $\lambda = 0$, with a loading coefficient $C = 0.02$.

We define our collocation scheme by choosing $M=7$, with the corresponding "shape collocation points",

$$x_j = 0.03, 0.1, 0.25, 0.5, 0.9, 1.5, 2.5$$

for $j=1, \dots, 7$ respectively; and $N=9$, with the corresponding "gamma collocation points",

$$x_j = 0.02, 0.05, 0.1, 0.18, 0.3, 0.5, 0.85, 1.4, 2.5$$

for $j=1, \dots, 9$. We emphasize that there is little point in choosing collocation points further downstream than $x = 2.5$, say, since (as we will see in the subsequent Figures) the flow at that station is essentially identical to that in the ultimate jet. In fact, it can be expected to lead to an ill-conditioned set of equations since our expression (43) for γ automatically satisfies the dynamic equation at infinity. As a final word of caution we note

that $x=0$ must not be included as a gamma collocation point since the dynamic equation is not satisfied at $x=0$.

As our "matching functions" we choose

$$f_j(x) = e^{-jx} \quad (48)$$

$$\begin{aligned} g_j(x) &= x^{-\frac{1}{2}} e^{-3x} \quad , \quad j=1 \\ &= x^{-0.84+0.51j} e^{-3x} \quad , \quad j \geq 2 \end{aligned} \quad (49)$$

as shown in Fig. 6. These were arrived at by trial and error, and appear to be equally suitable for all values $\lambda \geq 0$ and $C > 0$.

Starting with $T^{(0)} = 1$ and $\gamma_s^{(0)} = 0.1411$ (from (31) and (32)), and setting the damping factor $\alpha = 1.8$, the iteration is found to be rapidly convergent, as shown in Figs. 7-12. As our convergence criterion, we required the iteration to continue until $T^{(n+1)}$ and $\gamma_s^{(n+1)}$ agreed with their previous values, $T^{(n)}$ and $\gamma_s^{(n)}$, to within 0.6% at each of the x values listed in Figs. 8-12. Although it took five iterations to achieve this condition, it is seen that even the second iterate provides a fairly good uniform approximation to the solution.

However, it remains to show that the converged results do, in fact, represent the solution - since we only required satisfaction of the equations at several discrete collocation points. To settle this point, we have included a numerical check in the program (Appendix), which actually compares the left and right hand sides of the kinematic and dynamic equations (23) and (22). The results of this check indicate (Fig. 13) uniformly good agreement.

The flow field has also been computed, and is shown in Fig. 14. It is important to note that for the static condition the streamline pattern is virtually independent of C , at least over the range of values which are of practical interest. To see this, consider the governing equations (23) and (24). For $\lambda=0$, the C dependence cancels out of (23) since both Ψ_∞ and γ are proportional to γ_∞ which, in turn, contains the C dependence. Turning to the dynamic equation (24), we see that if we discard the swirl term $C^2/8T^2$, γ will (for $\lambda=0$) simply be proportional to $C^{\frac{1}{2}}$. With the swirl term omitted, then, it follows that the streamline pattern will be completely independent of C although, of course, the velocities will be proportional to $C^{\frac{1}{2}}$. With the swirl term included, this result is no longer true in an exact sense. However, for practical values of C , $C^2/8T^2 \ll C/2$ in (24), so that our statement nevertheless remains true in an approximate sense. To verify this numerically, we re-computed our numerical example with C increased by eight times, i.e. with $C=0.16$, and found the streamlines to be virtually unchanged!

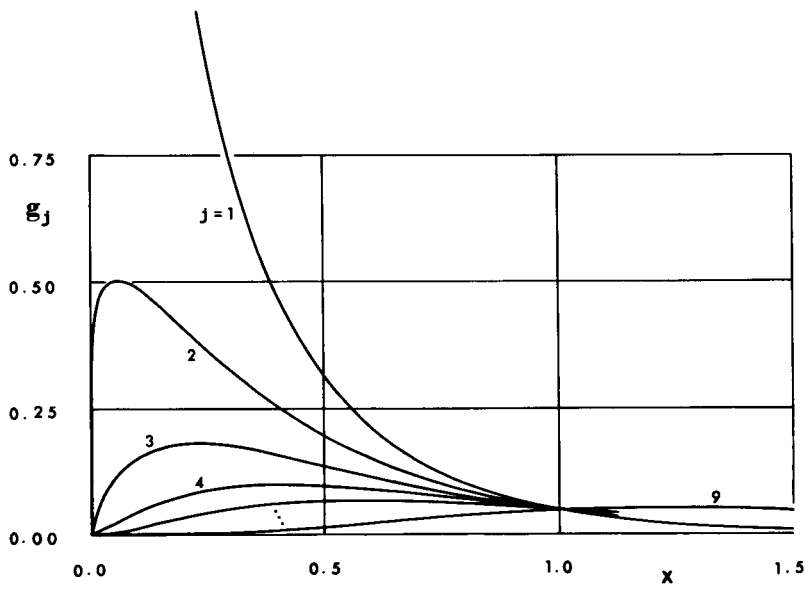
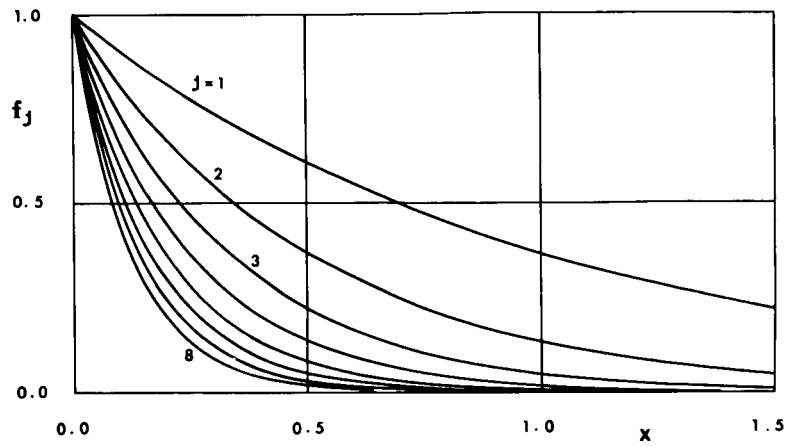


Figure 6. The Matching Functions

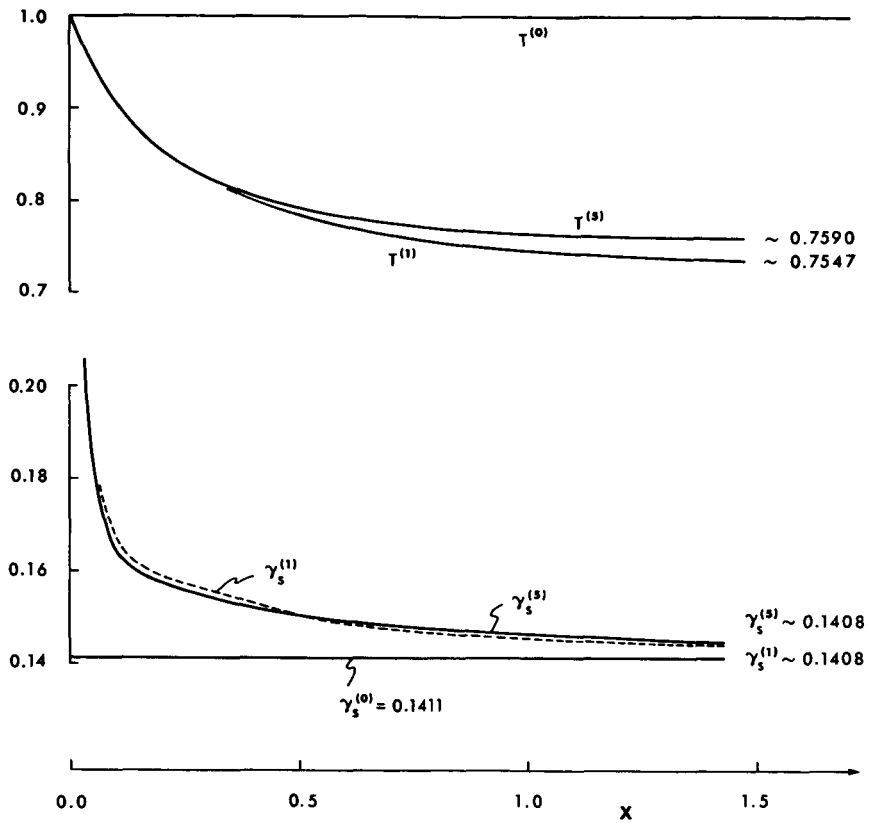


Figure 7. Successive Iterates for Numerical Example

ITERATION NO. 1

SHAPE COEFFICIENTS		GAMMA COEFFICIENTS		X	SLIPSTREAM RADIUS, Y	SLIPSTREAM CIRCULATION GAMMA SUB S
B SUB 1 #	-1.6159	A SUB 1 #	0.933	0.00	1.0000	INFINITY
B SUB 2 #	5.1913	A SUB 2 #	7.019	0.01	.9873	.2792
B SUB 3 #	-19.5532	A SUB 3 #	-7.6336	0.30	.9645	.2102
B SUB 4 #	39.7679	A SUB 4 #	26.9076	0.50	.9446	.1875
B SUB 5 #	-43.3864	A SUB 5 #	-45.3438	0.70	.9272	.1762
B SUB 6 #	23.7830	A SUB 6 #	54.8806	1.00	.9021	.1675
B SUB 7 #	-4.9614	A SUB 7 #	-59.9943	1.30	.8763	.1615
		A SUB 8 #	44.1277	2.00	.8544	.1590
		A SUB 9 #	-13.0430	2.50	.8371	.1574
				3.00	.8230	.1560
				4.00	.8010	.1531
				5.00	.7846	.1505
				6.00	.7722	.1486
				7.00	.7631	.1473
				8.00	.7564	.1465
				9.00	.7515	.1460
				1.0000	.7478	.1457
				1.250	.7411	.1448
				1.500	.7359	.1436
				1.750	.7319	.1423
				2.000	.7295	.1412
				2.250	.7290	.1405
				2.500	.7300	.1401
				2.750	.7321	.1401
				3.000	.7347	.1401
				4.000	.7451	.1406
				5.000	.7508	.1408
				6.000	.7532	.1408
				7.000	.7542	.1408
				8.000	.7545	.1408
				INFINITY	.7547	.1408

UNIFORM ACCURACY OF .6000 PERCENT IS NOT ATTAINED FOR SLIPSTREAM RADIUS AND CIRCULATION DISTRIBUTIONS.
AT MOST 6 MORE ITERATION(S) WILL BE ATTEMPTED.

Figure 8. Computer Print-Out for Numerical Example; Iteration No. 1

ITERATION NO. 2

SHAPE COEFFICIENTS		GAMMA COEFFICIENTS		X	SLIPSTREAM RADIUS, T	SLIPSTREAM CIRCULATION GAMMA SUB S
B SUB 1 =	.1630	A SUB 1 =	.1394	.000	1.0000	INFINITY
B SUB 2 =	-2.0314	A SUB 2 =	-.9966	.010	.9897	.2849
B SUB 3 =	9.8344	A SUB 3 =	2.7803	.030	.9606	.2012
B SUB 4 =	-24.6468	A SUB 4 =	-8.3600	.050	.9394	.1790
B SUB 5 =	34.7424	A SUB 5 =	46.0351	.070	.9213	.1693
B SUB 6 =	-25.5606	A SUB 6 =	-127.7351	.100	.8988	.1628
B SUB 7 =	7.7311	A SUB 7 =	171.6066	.150	.8708	.1567
		A SUB 8 =	-110.9082	.200	.8486	.1522
		A SUB 9 =	27.7593	.300	.8186	.1538
				.400	.7866	.1515
				.500	.7848	.1499
				.600	.7753	.1488
				.700	.7686	.1480
				.800	.7640	.1473
				.900	.7607	.1466
				1.000	.7583	.1460
				1.250	.7550	.1448
				1.500	.7540	.1441
				1.750	.7544	.1437
				2.000	.7550	.1435
				2.250	.7555	.1433
				2.500	.7557	.1430
				2.750	.7555	.1426
				3.000	.7551	.1422
				4.000	.7527	.1411
				5.000	.7511	.1408
				6.000	.7504	.1408
				7.000	.7501	.1408
				8.000	.7500	.1408
				INFINITY	.7499	.1408

UNIFORM ACCURACY OF .40000 PERCENT IS NOT ATTAINED FOR SLIPSTREAM RADIUS AND CIRCULATION DISTRIBUTIONS.
 AT MOST 5 MORE ITERATION(S) WILL BE ATTEMPTED.

Figure 9. Computer Print-Out for Numerical Example; Iteration No. 2

ITERATION NO. 3

SHAPE COEFFICIENTS	GAMMA COEFFICIENTS	X	SLIPSTREAM RADIUS, Y	SLIPSTREAM CIRCULATION GAMMA SUB S
B SUB 1 = .0287	A SUB 1 = .1420	.000	1.0000	INFINITY
B SUB 2 = -.4209	A SUB 2 = -1.0409	.000	.9842	.2885
B SUB 3 = 2.8560	A SUB 3 = 3.2076	.000	.9616	.9034
B SUB 4 = -8.9825	A SUB 4 = -10.2344	.050	.9410	.8805
B SUB 5 = 15.5383	A SUB 5 = 46.0189	.070	.9233	.8704
B SUB 6 = -13.3981	A SUB 6 = -112.1238	.100	.9011	.8635
B SUB 7 = 4.5818	A SUB 7 = 137.3062	.150	.8728	.8591
	A SUB 8 = -81.6722	.200	.8517	.8572
	A SUB 9 = 19.3796	.250	.8353	.8558
		.300	.8222	.8545
		.400	.8026	.8521
		.500	.7890	.8503
		.600	.7795	.8491
		.700	.7729	.8482
		.800	.7684	.8475
		.900	.7652	.8469
		1.000	.7629	.8464
		1.250	.7595	.8453
		1.500	.7578	.8444
		1.750	.7570	.8437
		2.000	.7567	.8432
		2.250	.7566	.8428
		2.500	.7566	.8424
		2.750	.7566	.8421
		3.000	.7565	.8417
		4.000	.7562	.8410
		5.000	.7560	.8408
		6.000	.7559	.8408
		7.000	.7559	.8408
		8.000	.7558	.8408
		INFINITY	.7558	.8408

UNIFORM ACCURACY OF .6000 PERCENT IS NOT ATTAINED FOR SLIPSTREAM RADIUS AND CIRCULATION DISTRIBUTIONS.
 AT MOST 4 MORE ITERATION(S) WILL BE ATTEMPTED.

Figure 10. Computer Print-Out for Numerical Example; Iteration No. 3

ITERATION NO. 4

SHAPE COEFFICIENTS		GAMMA COEFFICIENTS		X	SLIPSTREAM RADIUS, Y	SLIPSTREAM CIRCULATION GAMMA SUB S
B SUB 1 =	-0.535	A SUB 1 =	.1487	.000	1.0000	INFINITY
B SUB 2 =	-7.7122	A SUB 2 =	-9.9527	.010	.9864	.2910
B SUB 3 =	4.1050	A SUB 3 =	2.4768	.030	.9625	.2049
B SUB 4 =	-11.5929	A SUB 4 =	-6.3161	.050	.9421	.1817
B SUB 5 =	18.3790	A SUB 5 =	34.6208	.070	.9245	.1714
B SUB 6 =	-14.6818	A SUB 6 =	-95.2416	.100	.9126	.1642
B SUB 7 =	4.8900	A SUB 7 =	124.5816	.150	.8745	.1596
		A SUB 8 =	-77.6330	.200	.8535	.1575
		A SUB 9 =	19.1372	.250	.8371	.1559
				.300	.8240	.1546
				.400	.8044	.1522
				.500	.7909	.1505
				.600	.7814	.1492
				.700	.7748	.1483
				.800	.7702	.1476
				.900	.7669	.1469
				1.000	.7646	.1464
				1.250	.7612	.1452
				1.500	.7596	.1443
				1.750	.7591	.1438
				2.000	.7591	.1433
				2.250	.7592	.1429
				2.500	.7592	.1425
				2.750	.7592	.1422
				3.000	.7586	.1418
				4.000	.7586	.1410
				5.000	.7582	.1408
				6.000	.7580	.1408
				7.000	.7579	.1408
				8.000	.7579	.1408
				INFINITY	.7578	.1408

UNIFORM ACCURACY OF .60000 PERCENT IS NOT ATTAINED FOR SLIPSTREAM RADIUS AND CIRCULATION DISTRIBUTIONS.
 AT MOST 3 MORE ITERATION(S) WILL BE ATTEMPTED.

Figure 11. Computer Print-Out for Numerical Example; Iteration No. 4

ITERATION NO. 5

SHAPE COEFFICIENTS		GAMMA COEFFICIENTS		X	SLIPSTREAM RADIUS, r	SLIPSTREAM CIRCULATION GAMMA SUB S
B SUB 1 #	.0465	A SUB 1 #	1.434	.000	1.0000	INFINITY
B SUB 2 #	-.0370	A SUB 2 #	-.9322	.010	.9666	.2925
B SUB 3 #	3.7753	A SUB 3 #	2.2818	.030	.9629	.2059
B SUB 4 #	-10.0371	A SUB 4 #	5.2298	.050	.9427	.1824
B SUB 5 #	17.4260	A SUB 5 #	31.3733	.070	.9253	.1720
B SUB 6 #	-14.2465	A SUB 6 #	-88.9891	.100	.8636	.1648
B SUB 7 #	4.7138	A SUB 7 #	118.0818	.150	.8256	.1600
		A SUB 8 #	-74.2536	.200	.8547	.1577
		A SUB 9 #	18.3213	.250	.8384	.1561
				.300	.8253	.1547
				.400	.8057	.1523
				.500	.7921	.1505
				.600	.7826	.1492
				.700	.7760	.1483
				.800	.7714	.1476
				.900	.7681	.1470
				1.000	.7658	.1464
				1.250	.7623	.1452
				1.500	.7608	.1444
				1.750	.7602	.1438
				2.000	.7601	.1433
				2.250	.7601	.1429
				2.500	.7602	.1425
				2.750	.7602	.1421
				3.000	.7602	.1418
				4.000	.7597	.1410
				5.000	.7593	.1408
				6.000	.7591	.1408
				7.000	.7591	.1408
				8.000	.7590	.1408
				INFINITY	.7590	.1408

UNIFORM ACCURACY OF .6000 PERCENT IS ATTAINED FOR SLIPSTREAM RADIUS AND CIRCULATION DISTRIBUTIONS. ITERATION IS TERMINATED. DYNAMIC AND KINEMATIC CONDITIONS ON STREAMLINE WILL BE CHECKED AND FLOW PATTERN COMPUTED.

Figure 12. Computer Print-Out for Numerical Example; Iteration No. 5

X	TOTAL X-VEL. ON SLIPSTREAM, U(X)		SLIPSTREAM VORTICITY PER UNIT X-LENGTH, GAMMA(X)		DYNAMIC, U*GAMMA SHOULD EQUAL F/2		KINEMATIC, TOTAL (CAP) PSI ON SLIPSTREAM SHOULD EQUAL ITS VALUE AT X-INFINITY	
	LMS	RMS	LMS	RMS	LMS	RMS	LMS	RMS
.01	.02116	.47632	.01008	.00995	.01008	.00995	.04048	.04056
.02	.02771	.35891	.00995	.00995	.00995	.00995	.04061	.04056
.03	.03275	.30479	.00998	.00995	.00998	.00995	.04063	.04056
.04	.03664	.27282	.00997	.00994	.00997	.00994	.04062	.04056
.05	.03983	.24983	.00994	.00994	.00994	.00994	.04060	.04056
.10	.05051	.19676	.00994	.00993	.00994	.00993	.04059	.04056
.15	.05602	.17734	.00993	.00993	.00993	.00993	.04059	.04056
.20	.05910	.16799	.00993	.00993	.00993	.00993	.04059	.04056
.30	.06244	.15897	.00992	.00992	.00992	.00992	.04057	.04056
.40	.06530	.15429	.00992	.00992	.00992	.00992	.04057	.04056
.50	.06780	.15146	.00991	.00991	.00991	.00991	.04056	.04056
.75	.06977	.14889	.00991	.00991	.00991	.00991	.04056	.04056
1.00	.06789	.14645	.00991	.00991	.00991	.00991	.04058	.04056
1.25	.06826	.14524	.00991	.00991	.00991	.00991	.04057	.04056
1.50	.06888	.14437	.00991	.00991	.00991	.00991	.04057	.04056
2.00	.06913	.14330	.00991	.00991	.00991	.00991	.04058	.04056
3.00	.06948	.14181	.00985	.00991	.00985	.00991	.04051	.04056
5.00	.06982	.14084	.00983	.00991	.00983	.00991	.04039	.04056
10.00	.07017	.14081	.00988	.00991	.00988	.00991	.04045	.04056
INF.	.07040	.14081	.00991	.00991	.00991	.00991	.04056	.04056

Figure 13. Computer Print-Out for Numerical Example; Numerical Check

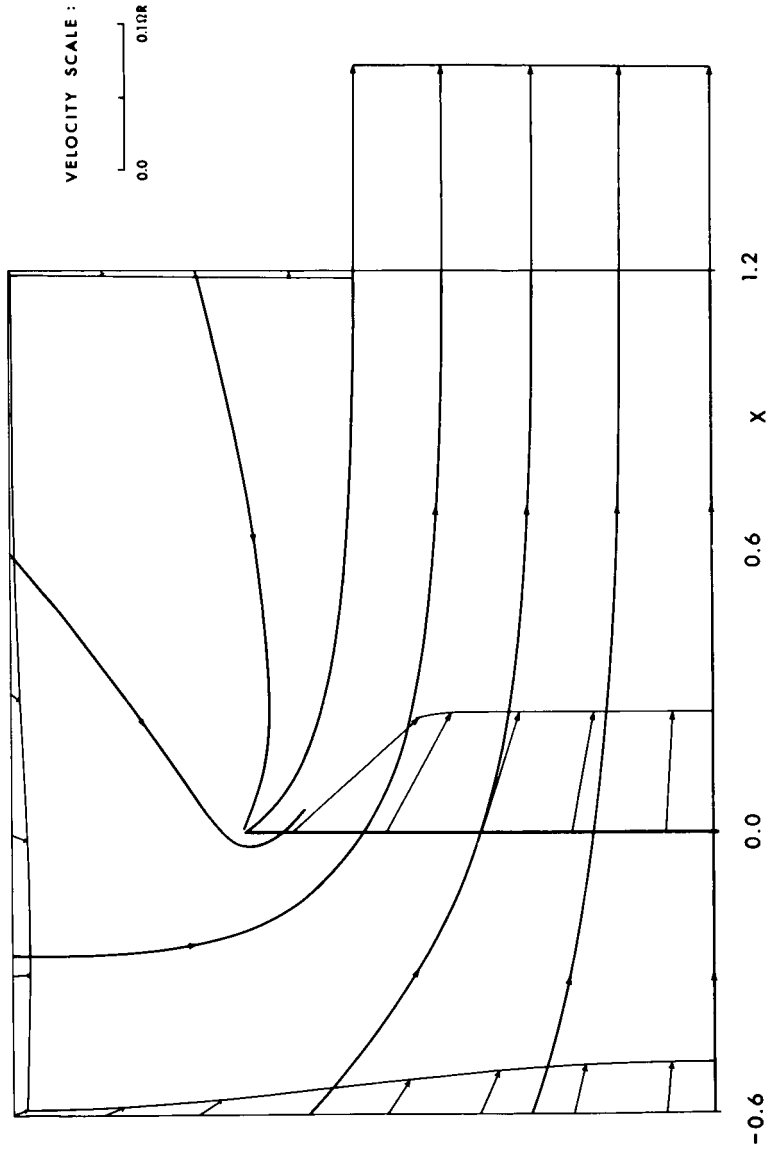


Figure 14. Resulting Flow Field for Numerical Example

Two points are of special interest with regard to Fig. 14 . First, we point out that at $x=1.2$ the (meridional) velocity inside the slipstream is almost constant, and is only about one percent smaller than its ultimate value at $x=\infty$.

Second, we see that the x -component of velocity is almost exactly constant over the actuator disk - out to about $r=0.9$ where it starts to drop off. As r increases further, the trend must reverse since the axial velocity must $\rightarrow \infty$ as $r \rightarrow 1^-$ by virtue of the square-root singularity in γ at the lip. Now, it is known (e.g. Reference 8) that in the light loading limit (i.e. the linearized actuator disk theory), the axial component of the induced velocity is exactly constant over the disk radius. The fact that this result is born out over most of the disk radius in our example, which is at the other (nonlinear) extreme, leads us to wonder whether the axial component of the induced velocity is in fact exactly constant over the disk radius (for our case $\Gamma(r) = \text{constant}$), for any condition between (and including) the lightly loaded and static limits.

If this were true, it would imply that our initial slipstream contraction must be purely radial! This follows immediately from the fact that the meridional velocity is infinite just inside the lip, due to the square-root singularity in γ . Its inclination must therefore be radial if the axial velocity is to remain constant at $x=0$ as $r \rightarrow 1^-$.

Flow visualization studies (References 9,10) (for a finite blade number, of course) do indicate a strong radial flow in the tip region. Instead of purely radial flow, in fact, Reference 10 reports a slight upstream inclination of the flow at the tip, so that a reverse flow exists over approximately the outer 5% of the blade radius. We must note, however, that the existing $\Gamma(r)$ in Reference 10 is undoubtedly quite unlike our prescribed distribution, $\Gamma(r) \equiv \text{constant}$, especially near the tip.

On the other hand, if the axial component of the induced velocity is not exactly constant over the disk radius then the strongly nonuniform axial inflow in the tip region is in fact correct, and may have a bearing on the well-known double bump in spanwise loading which has been observed near the tip of a number of helicopter rotors.

In any case, it seems clear that our results (Figs. 7-14) are quite accurate except, possibly, in the immediate tip region. The details in this region remain to be clarified.

Inclusion of the Ground Effect

The Integral Equations. Three changes are required in the integral equations (23) and (24) in order to accommodate the effect of a ground plane at $x=X$; see Fig. 15 . First of all they contain an arbitrary advance ratio λ ,

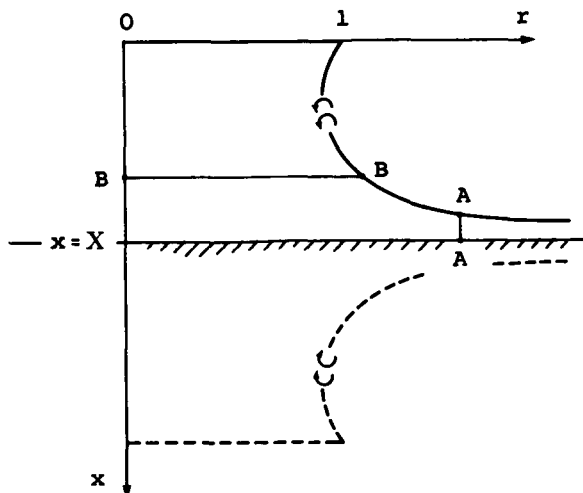


Figure 15. Ground Effect Model

whereas in the ground effect case we limit ourselves to static hover, so that $\lambda = 0$. In addition, we change the upper integration limits to X , and modify the Green's function so that it satisfies the additional boundary condition $u = 0$ at the ground plane. Specifically, we now have

$$G = T^{\frac{1}{2}} t^{\frac{1}{2}} [Q_{\frac{1}{2}}(\tilde{\omega}_2) - Q_{\frac{1}{2}}(\tilde{\omega}_2)] / 2\pi \quad (50)$$

where $\tilde{\tilde{\omega}}_2$ is identical to $\tilde{\omega}_2$, with $(x - \xi)^2$ replaced by $(x - 2X + \xi)^2$. Interpreted in terms of a vortex model, this amounts to adding an image system as indicated by the dashed lines in Fig. 15.

Analogous to equations (27) and (28), we now have

$$G_T = [A Q_{\frac{1}{2}}(\tilde{\omega}_2) + B Q_{-\frac{1}{2}}(\tilde{\omega}_2)] / (\tilde{\omega}_2^2 - 1) - [\tilde{A} Q_{\frac{1}{2}}(\tilde{\tilde{\omega}}_2) + \tilde{B} Q_{-\frac{1}{2}}(\tilde{\tilde{\omega}}_2)] / (\tilde{\tilde{\omega}}_2^2 - 1) \quad (51)$$

where \tilde{A} and \tilde{B} are identical to A and B , with $(x - \xi)^2$ replaced by $(x - 2X + \xi)^2$.

We observe that as $X \rightarrow \infty$, $\tilde{\tilde{\omega}}_2$ and $Q_{\pm \frac{1}{2}}(\tilde{\tilde{\omega}}_2)$ all tend to zero so that we do recover our previous out-of-ground-effect equations.

Asymptotic Behavior Near the Ground Plane. As $x \rightarrow X^-$, we see from (19) and (22) that $\gamma_s \xi \sim c/2$ since $t \rightarrow \infty$ in the denominator of the last term in (22). In addition, we must have $\xi \sim \gamma_s/2$, the drift velocity induced on the slipstream by the image vortex sheet. Combining these results, it follows that $\gamma_s \sim c^{\frac{1}{2}}$.

To obtain the asymptotic behavior of T , we apply the continuity equation at an arbitrary station AA, as shown in Fig. 15. The "control area" is $(2\pi T)(X-x)$ and the velocity through it is $\sim \gamma_s$; $\gamma_s/2$ due to the slipstream vorticity, and $\gamma_s/2$ due to the image vorticity. Continuity therefore requires that $\gamma_s(2\pi T)(X-x) = \text{constant}$ and, recalling that $\gamma_s \sim c^{\frac{1}{2}}$, it follows that $T(x) \sim O(X-x)^{-1}$.

In order to incorporate this behavior explicitly, we expand

$$T^{(n)}(x) = 1 + \sum_{j=1}^M [h_j(x) - h_j(0)] b_j^{(n)} \quad (52)$$

$$\gamma^{(n)}(x) = \sqrt{-^{(n)}} \gamma_s^{(n)}(x) = \sqrt{-^{(n)}} c^{\frac{1}{2}} \left\{ 1 + \sum_{j=1}^N g_j(x) a_j^{(n)} \right\} \quad (53)$$

where $h_j(x) = f_j(x)/(X-x)$ and the g_j 's tend to zero as $x \rightarrow X$; c.f. equations (42) and (43) for the out-of-ground-effect limit.

The Final Equations. Linear algebraic equations analogous to (44) and (45) can be obtained almost exactly as before. The only difference is in the expression of " Ψ_∞ ". Since $2\pi\Psi_\infty$ is the mass flow rate through any disk BB (see Fig. 15) it is also, by continuity, the flow rate through the asymptotic station AA; namely, $\gamma_s(2\pi T)(X-x)$. Instead of (35), therefore, we have

$$\Psi_\infty^{(n+1)} = c^{\frac{1}{2}} \sum_{j=1}^M f_j(X) b_j^{(n+1)} \quad (54)$$

Using $\beta=0$ again, we find that our kinematic equation can be reduced to

$$\begin{aligned} & \int_0^X \left\{ -G^{(n)} + \alpha(T^{(n)} - 1)G_T^{(n)} \right\} \gamma^{(n)} d\xi \\ &= \sum_{j=1}^M \left\{ \alpha[h_j(x) - h_j(0)] \int_0^X G_T^{(n)} \gamma^{(n)} d\xi - c^{\frac{1}{2}} f_j(X) \right\} b_j^{(n+1)} \end{aligned} \quad (55)$$

for $n=0, 1, \dots$, and for the dynamic equation we obtain

$$\left[\frac{\gamma_s^{(n)}}{c^{\frac{1}{2}}} - \frac{1}{2} \right] \frac{T^{(n+1)} F^{(n+1)}}{\sqrt{-(n+1)\gamma_s^{(n)}} 2} - \int_0^X G_T^{(n+1)} \sqrt{-(n+1)} d\xi$$

$$= \sum_{j=1}^N \left\{ \frac{T^{(n+1)} F^{(n+1)} g_j}{2\sqrt{-(n+1)\gamma_s^{(n)}}} + \int_0^X G_T^{(n+1)} \sqrt{-(n+1)} g_j d\xi \right\} a_j^{(n+1)} \quad (56)$$

Our procedure is the same as it was with equations (44) and (45); starting with $n=0$ we compute the $b_j^{(1)}$'s by satisfying (55) at M collocation points, the $a_j^{(1)}$'s by satisfying (56) at N collocation points, and so on, in turn, until convergence is attained.

Numerical Results. Let us consider, for example, the case where $X=1$ and $c=0.02$.

We fix our collocation scheme by choosing $M=6$, with the corresponding shape collocation points

$$x_j = 0.03, 0.1, 0.25, 0.45, 0.65, 0.9$$

for $j=1, \dots, 6$ respectively; and $N=1$, for simplicity, with the corresponding gamma collocation point $x_1 = 0.1$.

As our matching functions we choose

$$f_j(x) = x^j, \quad j = 1, \dots, 6 \quad (57)$$

$$g_j(x) = x^{-\frac{1}{2}}(X-x)^2, \quad j = 1 \quad (58)$$

The form of g_1 ensures the satisfaction of both end conditions; $\gamma_s = O(x^{-\frac{1}{2}})$ as $x \rightarrow 0$ and $\gamma_s \sim c^{\frac{1}{2}}$ as $x \rightarrow X$.

Starting with $a_1^{(0)} = 0$, $b_2^{(0)} = 0.1$ and $b_j^{(0)} = 0$ for $j \neq 2$, the iteration is found to be more slowly convergent than in the out-of-ground-effect case. The streamline pattern and slipstream shape corresponding to the eighth iterate, which appears to have settled down to within about one percent, are shown in Fig. 16; the shape collocation points are indicated (on the slipstream) by dots. The corresponding slipstream vorticity is defined by the value $a_1^{(8)} = 0.022$, so that

$$\gamma_s^{(8)} = c^{\frac{1}{2}}[1 + 0.022x^{-\frac{1}{2}}(1-x)^2] \quad (59)$$

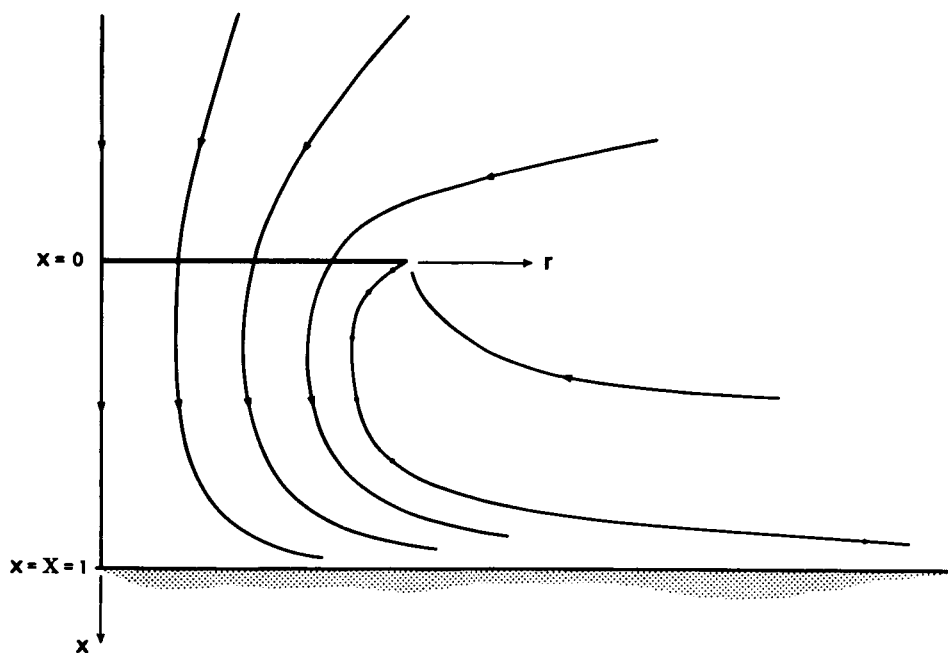


Figure 16. Resulting Flow Field for Numerical Example

Qualitatively, the results in Fig. 16 appear to be quite reasonable compared with the smoke visualization studies of Fradenburgh (Reference 11) - except for the absence of a dead-air dome beneath the hub, predicted by Heyson (Reference 12) and observed by Fradenburgh. This is to be expected, however, since our blade circulation is assumed to be constant all the way down to $r = 0^+$, so that there are no trailing vortices of reverse strength emitted over the inboard portion of the blades.

Quantitatively, we hesitate to claim a level of accuracy comparable to that obtained in the out-of-ground-effect case since only a single gamma collocation point was used. We did, in fact, run cases with $N=6$ or more, but unsatisfactory "wiggles" began to appear in both γ_s and T . We attribute this to our inability to prescribe a sufficiently "natural" family of g_j matching functions.

We point out that our previous statement "For the static condition the streamline pattern is virtually independent of C ", pertaining to the out-of-ground-effect case, is equally valid for the ground-effect case.

CONCLUSIONS

The inviscid flow field induced by a rotor in ground effect is found, based upon an actuator disk model with a constant circulation distribution. The governing nonlinear integral equations are solved by a systematic iterative scheme which is similar to the Newton-Raphson method for the solution of nonlinear algebraic equations.

First, the out-of-ground-effect limit is considered in detail. The iteration is found to be rapidly convergent and the results are shown to be quite accurate, except possibly in the immediate neighborhood of the blade tips. Specifically, there is some question as to whether or not the axial inflow should be constant over the blade radius or, equivalently, whether or not the initial slipstream contraction should be purely radial. This point is of some importance because of the square-root singularity in the slipstream vorticity at the "lip" of the slipstream. That is, the axial inflow (which is crucial from the point of view of blade design) through the tip portion of the blade will be bounded if the initial contraction is purely radial, and unbounded if it is not! In any case, it seems clear that our results are quite accurate except, possibly, in the immediate neighborhood of the blade tip.

Results for the ground effect case look entirely reasonable compared with the flow visualization studies of Fradenburgh (Reference 11), although we cannot claim a level of accuracy as high as in the out-of-ground-effect case.

In either case, in ground effect or not, it is shown that for the static condition the streamline pattern is virtually independent of the thrust coefficient

More precisely, it is exactly independent of the thrust coefficient - if the effects of swirl are neglected.

REFERENCES

1. Sowyrda, A., and DuWaldt, F. A., Representation of Wakes of Propellers in Ground Effect by Ring Vortex Systems, Cornell Aeronautical Laboratory Report No. BB-1665-S-1, April 1963 (DDC No. AD 602 988).
2. Brady, W. G., and Crimi, P., Representation of Propeller Wakes by Systems of Finite Core Vortices, Cornell Aeronautical Laboratory Report No. BB-1665-S-2, February 1965 (DDC No. AD 612 007).
3. DuWaldt, F. A., Representation of Propeller Wakes by Systems of Finite Core Vortices, Cornell Aeronautical Laboratory Report No. BB-1665-S-3, November 1966.
4. Scarborough, J. B., Numerical Mathematical Analysis, Sixth Edition, Johns Hopkins Press, Baltimore, 1966.
5. Wu, T. Y., Flow Through a Heavily Loaded Actuator Disk, Schiffstechnik, Vol. 9, No. 47, pp. 134-138, 1962.
6. Chaplin, H. R., A Method for Numerical Calculation of Slipstream Contraction of a Shrouded Impulse Disc in the Static Case With Application to Other Axisymmetric Potential Flow Problems, DTMB Aero Report 1077, 1964.
7. Watson, G. N., A Treatise on the Theory of Bessel Functions, Second Edition, Cambridge University Press, 1958.
8. Hough, G. R., and Ordway, D. E., The Generalized Actuator Disk, Developments in Theoretical and Applied Mechanics, Vol. II. Pergamon Press, Oxford/London/Edinburgh/New York/Paris/Frankfurt, 1965.
9. Taylor, M. K., A Balsa-Dust Technique for Air-Flow Visualization and its Application to Flow Through Model Helicopter Rotors in Static Thrust, NACA TN 2220, 1950.
10. Adams, G. N., Propeller Research at Canadair Limited, Proceedings of CAL/USAAVLABS Symposium on Aerodynamic Problems Associated with V/STOL Aircraft (Buffalo, New York, June 1966), Vol. 1.
11. Fradenburgh, E. A., Flow Field Measurements for a Hovering Rotor Near the Ground, Paper presented at the American Helicopter Society Fifth Annual Western Forum, Los Angeles, September 1958.
12. Heyson, Harry H., Induced Velocity Near a Rotor and its Application to Helicopter Problems, Proceedings of the 14th Annual National Forum, American Helicopter Society, April 1958.

APPENDIX

Listing of the Computer Codes

On the following pages are Fortran listings of the two computer codes, ROTORIGE (for the in-ground-effect case) and ROTOROGE (for the out-of-ground-effect case). Actually, the ROTORIGE code is presented for the special case where $N=1$, to be consistent with the numerical example in the text, and does not apply for $N \geq 2$.

Of the input variables (see the Common Statements in ROTORIGE) only "ACC" requires further description. If, for example, $ACC = 0.01$ the iteration will proceed until both $T^{(n+1)}$ and $\gamma^{(n+1)}$ agree with their previous values, $T^{(n)}$ and $\gamma^{(n)}$, at each of the print-out x's (e.g. Fig. 8) to within one percent or better - or until $n = "NITER"$, whichever occurs first.

Regarding the speed of the calculation, we point out that for the numerical examples presented in the text the machine time per iteration (on the CDC 1604) was 30 seconds for ROTORIGE, and one minute and 30 seconds for ROTOROGE.

PROGRAM ROTORIGE

```

C
C ROTOR IN GROUND EFFECT (NAS1-6349)
C FORMULATION USES ONE (1) COLLOCATION POINT FOR THE
C DYNAMIC (GAMMA) EQUATION.
C
C DEFINITION OF INPUT VARIABLES
C IM = MONTH OF YEAR IN INTEGER FORM.
C ID = DAY OF MONTH IN INTEGER FORM.
C IY = LAST TWO DIGITS OF YEAR IN INTEGER FORM.
C MM = NO. OF COLLOCATION POINTS FOR SHAPE EQUATION.
C NN = NO. OF COLLOCATION POINTS FOR GAMMA EQUATION.
C NITER = MAXIMUM NO. OF ITERATIONS TO BE ATTEMPTED.
C CC = LOADING COEFFICIENT.
C CAPX = NON-DIMENSIONAL DISTANCE FROM GROUND PLANE TO PROPELLER PLANE.
C ACC = CONVERGENCE CRITERION IN PERCENT/100
C XS = NON-DIMENSIONAL AXIAL COORDINATES OF SHAPE COLLOCATION POINTS.
C XG = NON-DIMENSIONAL AXIAL COORDINATES OF GAMMA COLLOCATION POINTS.
C B = INITIAL SHAPE COEFFICIENTS.
C A = INITIAL GAMMA COEFFICIENTS.
C
C
C EXTERNAL FJ
C TYPE REAL LHS
C COMMON/ADDED/FZ(50)
C COMMON/COEFS/A(50),B(50)
C COMMON/INPUT/CC,ALPHA,CAPX
C COMMON/INTGND/NGEES,TT,ZZ,N,K
C COMMON/MATRIX/RHS(50,50),LHS(50,1)
C COMMON/NUMBERXS/NXS,NXG
C COMMON/PRINT/XS(50),XG(50),XP(50),SR(50),SC(50),ITER,IM,ID,IY
C COMMON/SAVE/NP,INDEX,SRS(50),SCS(50)
1000 FORMAT(4I5)
1010 FORMAT(10F8.5)
1020 FORMAT(1H0,2BHINITIAL CONDITIONS - AT MOST,13,14H ITERATION(S) ,
* 18HWILL BE ATTEMPTED.)
1030 FORMAT(1H0,19HUNIFORM ACCURACY OF,F8.5,16H PERCENT IS NOT ,
* 47HATTAINED FOR SLIPSTREAM RADIUS AND CIRCULATION ,
* 14HDISTRIBUTIONS.,/,8H AT MOST,13,19H MORE ITERATION(S) ,
* 18HWILL BE ATTEMPTED.)
1040 FORMAT(1H0,19HUNIFORM ACCURACY OF,F8.5,12H PERCENT IS ,
* 47HATTAINED FOR SLIPSTREAM RADIUS AND CIRCULATION ,
* 14HDISTRIBUTIONS.,/,25H ITERATION IS TERMINATED.)
1050 FORMAT(1H0,19HUNIFORM ACCURACY OF,F8.5,16H PERCENT IS NOT ,
* 47HATTAINED FOR SLIPSTREAM RADIUS AND CIRCULATION ,
* 14HDISTRIBUTIONS.,/,25H ITERATION IS TERMINATED.)
READ 1000,IM,ID,IY
10 READ 1000,MM,NN,NITER $ IF (MM) 150,150,20
20 READ 1010,CC,CAPX,ACC
READ 1010,(XS(I),I=1,MM) $ READ 1010,(XG(I),I=1,NN)
NXS=MM $ NXG=NN
READ 1010,(B(I),I=1,NXS) $ READ 1010,(A(I),I=1,NXG)
ALPHA=1.8
DO 30 I=1,NXS
FZ(I)=FJ(0.0,I)
30 CONTINUE
ITER=0 $ ACCP=100.0*ACC
INDEX=1 $ CALL OUTPUT
INDEX=2 $ PRINT 1020,NITER
DO 120 ITER=1,NITER
N=NXS

```

```

DO 40 I=1,N
ZZ=XS(I)                $ CALL TOPBOT(ZZ)
CALL LIMITCHK           $ CALL BEQNS(I)
40 CONTINUE
CALL MATINV(RHS,N,LHS,I,DET)
DO 50 J=1,N
B(J)=LHS(.,1)
50 CONTINUE
N=NXG
DO 60 I=1,N
ZZ=XG(I)                $ CALL TOPBOT(ZZ)
CALL LIMITCHK           $ CALL AEQNS(I)
60 CONTINUE
CALL ACOEFS
CALL OUTPUT
DO 90 I=2,NP
CACC=ACC*SC(I)          $ TACC=ACC*SR(I)
IF (ABSF(SC(I)-SCS(I))-CACC) 80,80,100
80 IF (ABSF(SR(I)-SRS(I))-TACC) 90,90,100
90 CONTINUE
GO TO 130
100 LEFT=NITER-ITER     $ IF (LEFT) 140,140,110
110 PRINT 1030,ACCP,LEFT
120 CONTINUE
130 PRINT 1040,ACCP     $ GO TO 10
140 PRINT 1050,ACCP     $ GO TO 10
150 END

```

```

SUBROUTINE ACOEFS
COMMON/ASPEC/AJ(2),AK(2),AL(2),FZZ,GZZ,AZZ,BZZ
COMMON/COEFS/A(50),B(50)
TOP=-AK(1)+SORTF(AK(1)**2-4.0*AJ(1)*AL(1))
BOT=2.0*AL(1)           $ A(1)=TOP/BOT
END

```

```

SUBROUTINE AEQNS(I)
EXTERNAL AJINT,AKINT,ALINT
EXTERNAL GJ
COMMON/ASPEC/AJ(2),AK(2),AL(2),FZZ,GZZ,AZZ,BZZ
COMMON/COEFS/A(50),B(50)
COMMON/INPUT/CC,ALPHA,CAPX
COMMON/INTGND/NGEES,TT,ZZ,N,K
CALL SHAPE(ZZ,TT)      $ CALL FACTOR(ZZ,FZZ)
GZZ=GJ(ZZ)             $ FF=CC-(CC/(2.0*TT))**2
AJ(I)=-FF*TT/(2.0*CC*FZZ) $ AK(I)=AL(I)=0.0
CALL ONEINTGL(AJINT,AJ(I)) $ CALL ONEINTGL(AKINT,AK(I))
CALL ONEINTGL(ALINT,AL(I))
END

```

```

FUNCTION AJINT(Z)
COMMON/ASPEC/AJ(2),AK(2),AL(2),FZZ,GZZ,AZZ,BZZ
COMMON/INTGND/NGEES,TT,ZZ,N,K
CALL SHAPE(Z,T)        $ CALL FACTOR(Z,FZ)
CALL GEES(1,TT,T,ZZ,Z,G,GTT) $ AJINT=GTT*FZ
END

```

```

FUNCTION AKINT(Z)
EXTERNAL GJ
COMMON/ASPEC/AJ(2),AK(2),AL(2),FZZ,GZZ,AZZ,BZZ
COMMON/INTGND/NGEES,TT,ZZ,N,K
CALL SHAPE(Z,T)           $ CALL FACTOR(Z,FZ)
CALL GEES(1,TT,T,ZZ,Z,G,GTT) $ AKINT=GTT*FZ*(GZZ+GJ(Z))
END

```

```

FUNCTION ALINT(Z)
EXTERNAL GJ
COMMON/ASPEC/AJ(2),AK(2),AL(2),FZZ,GZZ,AZZ,BZZ
COMMON/INTGND/NGEES,TT,ZZ,N,K
CALL SHAPE(Z,T)           $ CALL FACTOR(Z,FZ)
CALL GEES(1,TT,T,ZZ,Z,G,GTT) $ ALINT=GTT*FZ*GZZ*GJ(Z)
END

```

```

SUBROUTINE BEGNS(I)
EXTERNAL BINT,FJ
TYPE REAL LHS
COMMON/ADDED/FZ(50)
COMMON/INPUT/CC,ALPHA,CAPX
COMMON/INTGND/NGEES,TT,ZZ,N,K
COMMON/MATRIX/RHS(50,50),LHS(50,1)
NN=N+1           $ CALL SHAPE(ZZ,TT)
GTTG=GGM=0.0
NGEES=1          $ CALL ONEINTGL(BINT,GTTG)
NGEES=3          $ CALL ONEINTGL(BINT,GGM)
DO 30 J=1,NN
K=J              $ IF (J-NN) 10,20,20
10 TERM=FJ(ZZ,K)/(CAPX-ZZ)-FZ(K)/CAPX
RHS(I,J)=-SQRTF(CC)*FJ(CAPX,J)+ALPHA*TERM*GTTG
GO TO 30
20 RHS(I,J)=GGM+ALPHA*(TT-1.0)*GTTG
30 CONTINUE
LHS(I,1)=RHS(I,NN)
END

```

```

FUNCTION BINT(Z)
EXTERNAL FJ
COMMON/ADDED/FZ(50)
COMMON/INPUT/CC,ALPHA,CAPX
COMMON/INTGND/NGEES,TT,ZZ,N,K
CALL SHAPE(Z,T)           $ CALL VORTEX(Z,GAM)
CALL FACTOR(Z,FAC)        $ GAM=FAC*GAM
CALL GEES(NGEES,TT,T,ZZ,Z,G,GTT)
GO TO (10,30,20),NGEES
10 BINT=GTT*GAM           $ GO TO 30
20 BINT=-G*GAM
30 END

```

```

SUBROUTINE FACTOR(X,FAC)
EXTERNAL FJ,FPJ
COMMON/COEFS/A(50),B(50)
COMMON/INPUT/CC,ALPHA,CAPX
COMMON/NUMBERXS/NXS,NXG
TP=0.0           $ BOT=CAPX-X
DO 10 I=1,NXS
TP=TP+B(I)*(FPJ(X,I)/BOT+FPJ(X,I)/BOT**2)
10 CONTINUE
FAC=SQRTF(1.0+TP**2)
END

```

```

FUNCTION FJ(X,J)
FJ=X**J
END

```

```

FUNCTION FPJ(X,J)
IF (J-1) 10,10,20
10 FPJ=1.0
20 FPJ=J*X**(J-1)
30 END

```

```
$ GO TO 30
```

```

SUBROUTINE GEFS(NUM,TT,T,ZZ,Z,G,GTT)
COMMON/INPUT/CC,ALPHA,CAPX
PI=3.1415927
DX=(ZZ-Z)**2
DZ=(ZZ-2.0*CAPX+Z)**2
ARGA=1.0+(DT+DX)/(2.0*TERM**2)
ARGB=1.0+(DT+DZ)/(2.0*TERM**2)
GO TO (10,20,10),NUM
10 BOT=TT**2-T**2
BOTA=ARGA**2-1.0
AA=(DX+DT)*QPA/(BOT*T)
EE=(DZ+DT)*QPB/(BOT*T)
GTT=(AA+BB)/BOTA-(EE+DD)/BOTB
20 G=TERM*(QPA-QPB)/(2.0*PI)
30 END

```

```

$ DT=(TT-T)**2
$ TERM=SQRTF(TT*T)
$ CALL QPMHALF(ARGA,QPA,QMA)
$ CALL QPMHALF(ARGB,QPB,QMB)
$ BOT=8.0*PI*TERM
$ BOTB=ARGB**2-1.0
$ BB=(DX-DT)*QMA/(BOT*TT)
$ DD=(DZ-DT)*QMB/(BOT*TT)
$ GO TO (30,20,20),NUM

```

```

FUNCTION GGG(Z)
COMMON/INTGND/NGEES,TT,ZZ,N,K
CALL SHAPE(Z,T)
CALL FACTOR(Z,FAC)
CALL GEFS(2,TT,T,ZZ,Z,GG,DUM)
GGG=GG*G
END

```

```

$ CALL VORTEX(Z,G)
$ G=FAC*G

```

```

FUNCTION GJ(X)
COMMON/INPUT/CC,ALPHA,CAPX
GJ=(CAPX-X)**2/SQRTF(X)
END

```

```

SUBROUTINE LIMITCHK
COMMON/LIMITS/TOP(5),BOT(5),NGD(5)
DO 40 I=1,5
IF (BOT(I)-TOP(I)) 40,40,10
10 IF (I-5) 20,30,30
20 BOT(I+1)=BOT(I)
30 BOT(I)=TOP(I)
40 CONTINUE
END

```



```

SUBROUTINE MATINV(A,N,B,M,DETERM)
DIMENSION IPIVOT(50),A(50,50),B(50,1),INDEX(50,2),PIVOT(50)
DETERM=1.0
DO 10 J=1,N
IPIVOT(J)=0
10 CONTINUE
DO 200 I=1,N
AMAX=0.0
DO 60 J=1,N
IF (IPIVOT(J)-1) 20,60,20
20 DO 50 K=1,N
IF (IPIVOT(K)-1) 30,50,240
30 IF (ABS(A(J,K))-ABS(A(J,K))) 40,50,50
40 IROW=J $ ICOLUM=K
AMAX=A(J,K)
50 CONTINUE
60 CONTINUE
IPIVOT(ICOLUM)=IPIVOT(ICOLUM)+1 $ IF (IROW-ICOLUM) 70,110,70
70 DETERM=-DETERM
DO 80 L=1,N
SWAP=A(IROW,L) $ A(IROW,L)=A(ICOLUM,L)
A(ICOLUM,L)=SWAP
80 CONTINUE
IF (M) 110,110,90
90 DO 100 L=1,M
SWAP=B(IROW,L) $ B(IROW,L)=B(ICOLUM,L)
B(ICOLUM,L)=SWAP
100 CONTINUE
110 INDEX(I,1)=IROW
INDEX(I,2)=ICOLUM $ PIVOT(I)=A(ICOLUM,ICOLUM)
DETERM=DETERM*PIVOT(I) $ A(ICOLUM,ICOLUM)=1.0
DO 120 L=1,N
A(ICOLUM,L)=A(ICOLUM,L)/PIVOT(I)
120 CONTINUE
IF (M) 150,150,130
130 DO 140 L=1,M
B(ICOLUM,L)=B(ICOLUM,L)/PIVOT(I)
140 CONTINUE
150 DO 200 L1=1,N
IF (L1-ICOLUM) 160,200,160
160 T=A(L1,ICOLUM) $ A(L1,ICOLUM)=0.0
DO 170 L=1,N
A(L1,L)=A(L1,L)-A(ICOLUM,L)*T
170 CONTINUE
IF (M) 200,200,180
180 DO 190 L=1,M
B(L1,L)=B(L1,L)-B(ICOLUM,L)*T
190 CONTINUE
200 CONTINUE
DO 230 I=1,N
L=N+1-I
IF (INDEX(L,1)-INDEX(L,2)) 210,230,210
210 JROW=INDEX(L,1) $ JCOLUM=INDEX(L,2)
DO 220 K=1,N
SWAP=A(K,JROW) $ A(K,JROW)=A(K,JCOLUM)
A(K,JCOLUM)=SWAP
220 CONTINUE
230 CONTINUE
240 RETURN
END

```

```

SUBROUTINE NGAUSS(B,A,FX,NTIME,INTEGRAL)
TYPE REAL INTEGRAL
DIMENSION R(5),U(5)
DATA (R=0.1477621124,0.1346333597,0.1095431813,0.07472567458,
*      0.03333567215),
*      (U=0.0744371695,0.2166976971,0.3397047841,0.4325316833,
*      0.4869532643)
INTEGRAL=0.0
DO 20 J=1,NTIME
XL=A+(J-1)*(B-A)/NTIME          $ XU=B-(NTIME-J)*(B-A)/NTIME
D=XU-XL                          $ S=(XU+XL)/2.0
TEMP=0.0
DO 10 K=1,5
TEMP=TEMP+R(K)*(FX(S+D*U(K))+FX(S-D*U(K)))
10 CONTINUE
TEMP=TEMP*D                      $ INTEGRAL=INTEGRAL+TEMP
20 CONTINUE
END

```

```

SUBROUTINE ONEINTGL(FA,A)
COMMON/LIMITS/TOP(5),BOT(5),NGD(5)
DO 20 I=1,5
IF (ABS(TOP(I)-BOT(I))-0.0000001) 20,20,10
10 CALL NGAUSS(TOP(I),BOT(I),FA,NGD(I),AA)
A=A+AA
20 CONTINUE
END

```

```

SUBROUTINE OUTPUT
COMMON/ADDED/FZ(50)
COMMON/COEFS/A(50),B(50)
COMMON/INPUT/CC,ALPHA,CAPX
COMMON/INTGND/NGEES,TT,ZZ,N,K
COMMON/NUMBERXS/NXS,NXG
COMMON/PRINT/XS(50),XG(50),XP(50),SR(50),SC(50),ITER,IM,JD,IY
COMMON/SAVE/NP,INDEX,SRS(50),SCS(50)
1000 FORMAT(1H1,25X,32HR O T O R   I N   G R O U N D   ,
*      35HE F F E C T   ( N A S 1 - 6 3 4 9 ),5X,1H(,12,1H/,12,
*      1H/,12,1H))
1010 FORMAT(1H0,35X,29HDAMPING COEFFICIENTS, ALPHA =,F5.2,9H , BETA =,
*      4H 0.0,/,36X,
*      24HLOADING COEFFICIENT, C =,F7.4,/,36X,
*      16HHUB RADIUS = 0.0)
1020 FORMAT(1H0,21X,29HSHAPE COLLOCATION POINTS, M =,I3,12X,
*      29HGAMMA COLLOCATION POINTS, N =,I3,/)
1030 FORMAT(1H ,28X,5HX SUB,I3,2H =,F8.4,26X,5HX SUB,I3,2H =,F8.4)
1040 FORMAT(1H ,72X,5HX SUB,I3,2H =,F8.4)
1050 FORMAT(1H ,28X,5HX SUB,I3,2H =,F8.4)
1060 FORMAT(1H0,13HITERATION NO.,I3,/)
1070 FORMAT(1H ,79X,35HSLIPSTREAM   SLIPSTREAM CIRCULATION,/,7X,
*      18HSHAPE COEFFICIENTS,14X,18HGAMMA COEFFICIENTS,11X,1HX,
*      11X,30HRADIUS, T           GAMMA SUB S,/)
1071 FORMAT(1H ,4X,10HB SUB 1 =,F12.4,10X,10HA SUB 1 =,F12.4,8X,
*      4H,000,11X,6H1.0000,F18.4)
1072 FORMAT(1H ,4X,10HB SUB 1 =,F12.4,10X,10HA SUB 1 =,F12.4,8X,
*      4H,000,11X,6H1.0000,10X,8HINFINITY)
1080 FORMAT(1H ,4X,5HB SUB,I3,2H =,F12.4,10X,5HA SUB,I3,2H =,F12.4,
*      F12.3,F17.4,F18.4)
1090 FORMAT(1H ,4X,5HB SUB,I3,2H =,F12.4,10X,5HA SUB,I3,2H =,F12.4,
*      6HCAP X=,F6.3,9X,8HINFINITY,F18.4)
1100 FORMAT(1H ,4X,5HB SUB,I3,2H =,F12.4,10X,5HA SUB,I3,2H =,F12.4)
1110 FORMAT(1H ,4X,5HB SUB,I3,2H =,F12.4,32X,F12.3,F17.4,F18.4)

```

```

1120 FORMAT(1H ,4X,5HB SUB,I3,2H =,F12.4,32X,
*      6HCAP X=,F6.3,9X,8HINFINITY,F18.4)
1130 FORMAT(1H ,4X,5HB SUB,I3,2H =,F12.4)
1140 FORMAT(1H ,36X,5HA SUB,I3,2H =,F12.4,F12.3,F17.4,F18.4)
1150 FORMAT(1H ,36X,5HA SUB,I3,2H =,F12.4,
*      6HCAP X=,F6.3,9X,8HINFINITY,F18.4)
1160 FORMAT(1H ,36X,5HA SUB,I3,2H =,F12.4)
1170 FORMAT(1H ,58X,F12.3,F17.4,F18.4)
1180 FORMAT(1H ,58X,6HCAP X=,F6.3,9X,8HINFINITY,F18.4)
      NP=26
      DO 60 I=2,NP
      GO TO (5,4),INDEX
    4 SRS(I)=SR(I)          $ SCS(I)=SC(I)
      GO TO 50
    5 IF (I-5) 20,20,10
    10 IF (I-22) 30,30,40
    20 J=2*I-3              $ XP(I)=0.01*J
      GO TO 50
    30 J=I-4                $ XP(I)=0.05*J
      GO TO 50
    40 J=I-22               $ XP(I)=0.9+0.02*J
    50 CALL SHAPE(XP(I),SR(I)) $ CALL VORTEX(XP(I),SC(I))
    60 CONTINUE
    65 PRINT 1000,I,M,I0,IY $ PRINT 1010,ALPHA,CC
      PRINT 1020,NXS,NXG    $ IF (NXS-NXG) 70,70,80
    70 M=NXS                $ GO TO 90
    80 M=NXG
    90 PRINT 1030,(I,XS(I),I,XG(I),I=1,M)
      M=M+1                 $ IF (NXS-NXG) 100,120,110
    100 PRINT 1040,(I,XG(I),I=M,NXG) $ GO TO 120
    110 PRINT 1050,(I,XS(I),I=M,NXS)
    120 PRINT 1060,ITER     $ PRINT 1070
      IF (NXS-NXG) 130,140,140
    130 IF (NXG-NP) 150,150,160
    140 IF (NXS-NP) 150,150,170
    150 M=NP+1              $ GO TO 180
    160 M=NXG                $ GO TO 180
    170 M=NXS
    180 KOUNT=1              $ IF (ITER) 181,181,182
    181 TEMP=SQRTF(CC)     $ PRINT 1071,B(1),A(1),TEMP
      GO TO 183
    182 PRINT 1072,B(1),A(1)
    183 DO 390 I=2,M
      IF (I-NXS) 190,190,220
    190 IF (I-NXG) 200,200,210
    200 IF (I-NP) 250,250,260
    210 IF (I-NP) 290,290,300
    220 IF (I-NXG) 230,230,240
    230 IF (I-NP) 330,330,340
    240 IF (I-NP) 370,370,380
    250 PRINT 1080,I,B(I),I,A(I),XP(I),SR(I),SC(I)
      GO TO 390
    260 GO TO (270,280),KOUNT
    270 PRINT 1090,I,B(I),I,A(I),CAPX,TEMP
      KOUNT=2                $ GO TO 390
    280 PRINT 1100,I,B(I),I,A(I) $ GO TO 390
    290 PRINT 1110,I,B(I),XP(I),SR(I),SC(I)
      GO TO 390
    300 GO TO (310,320),KOUNT
    310 PRINT 1120,I,B(I),CAPX,TEMP
      KOUNT=2                $ GO TO 390
    320 PRINT 1130,I,B(I)    $ GO TO 390
    330 PRINT 1140,I,A(I),XP(I),SR(I),SC(I)
      GO TO 390
    340 GO TO (350,360),KOUNT

```

```

350 PRINT 1150,I,A(I),CAPX,TEMP          $ GO TO 390
      KOUNT=2                             $ GO TO 390
360 PRINT 1160,I,A(I)                   $ GO TO 390
370 PRINT 1170,XP(I),SR(I),SC(I)       $ GO TO 390
380 PRINT 1180,CAPX,TEMP
390 CONTINUE
      END

```

```

SUBROUTINE QPMHJLF(Z,QPH,QMH)
TYPE REAL KPRIMFSQ,K
KPRIMFSQ=1.0-(2.0/(Z+1.0))             $ A1=KPRIMFSQ
A2=A1*A1                               $ A3=A2*A1
A4=A2*A2                               $ ALO=LOGF(1.0/KPRIMFSQ)
K=SQRTF(2.0/(Z+1.0))                 $ B=SQRTF(2.0*(Z+1.0))
ELE=1.0000000000+.44325141463*A1+.06260601220*A2
*      +.04757383546*A3+.01736506451*A4+
*      (.24998368310*A1+.09200180037*A2+
*      .04069697526*A3+.00526449639*A4)*ALO
ELK=1.38629436112+.09666344259*A1+.03590092383*A2
*      +.03742563713*A3+.01451196212*A4+
*      (.50000000000+.12498593597*A1+.06880248576*A2
*      +.03328355346*A3+.00441787012*A4)*ALO
QPH=Z*K*ELK-B*ELE                      $ QMH=K*ELK
END

```

```

SUBROUTINE SHAPE(X,S)
EXTERNAL FJ
COMMON/ADDED/FZ(50)
COMMON/COEFS/A(50),B(50)
COMMON/INPUT/CC,ALPHA,CAPX
COMMON/NUMBERXS/NXS,NXG
S=1.0                                  $ BOT=CAPX-X
DO 10 J=1,NXS
S=S+(FJ(X,J)/BOT-FZ(J)/CAPX)*B(J)
10 CONTINUE
END

```

```

SUBROUTINE TOPBOT(ZZ)
COMMON/INPUT/CC,ALPHA,CAPX
COMMON/LIMITS/TOP(5),BOT(5),NGD(5)
TEMP=CAPX-0.12
DO 10 I=1,5
TOP(I)=BOT(I)=0.0                      $ NGD(I)=1
10 CONTINUE
IF (ABSF(ZZ)-0.0000001) 70,70,20
20 IF (ZZ) 70,70,30
30 IF (ABSF(ZZ-0.12)-0.0000001) 120,120,40
40 IF (ZZ-0.12) 80,120,50
50 IF (ABSF(ZZ-TEMP)-0.0000001) 120,120,60
60 IF (ZZ-TEMP) 120,120,130
70 TOP(1)=BOT(2)=0.1                    $ TOP(2)=BOT(3)=CAPX-0.1
TOP(3)=CAPX                            $ NGD(2)=2
GO TO 170
80 IF (ZZ-0.02) 90,90,100
90 EPS=ZZ                                $ GO TO 110
100 EPS=0.02
110 TOP(1)=BOT(2)=ZZ-EPS                $ TOP(2)=BOT(3)=ZZ+EPS
TOP(3)=BOT(4)=CAPX-0.1                 $ TOP(4)=CAPX
NGD(2)=3                                $ GO TO 170

```

```

120 TOP(1)=BOT(2)=0.10          $ TOP(2)=BOT(3)=ZZ-0.02
    TOP(3)=BOT(4)=ZZ+0.02      $ TOP(4)=BOT(5)=CAPX-0.1
    TOP(5)=CAPX                $ NGD(3)=3
    GO TO 170
130 IF (TEMP-0.02) 140,140,150
140 FPS=TEMP                    $ GO TO 160
150 FPS=0.02
160 TOP(1)=BOT(2)=0.1          $ TOP(2)=BOT(3)=ZZ-EPS
    TOP(3)=BOT(4)=Z7+FPS      $ TOP(4)=CAPX
    NGD(3)=3
170 END

```

```

SUBROUTINE VORTEX(X,V)
EXTERNAL GJ
COMMON/COEFS/A(50),B(50)
COMMON/INPUT/CC,ALPHA,CAPX
V=SQRTF(CC)*(1.0+A(1)*GJ(X))
END
      END      ROTORIGE
      FINIS

```

PROGRAM ROTORGE

C
C
C

ROTOR OUT OF GROUND EFFECT (NAS1-6349)

```

EXTERNAL FJ
TYPE REAL LHS,LAMBDA
COMMON/ADDED/FZ(50),TI
COMMON/COEFS/A(50),B(50)
COMMON/INPUT/LAMBDA,CC,ALPHA,BETA
COMMON/INTGND/NGEES,TT,ZZ,N,K,GI
COMMON/MATRIX/RHS(50,50),LHS(50,1)
COMMON/NUMBERXS/NXS,NXG
COMMON/PRINT/XS(50),XG(50),XP(50),SR(50),SC(50),ITER,IM,ID,IY
COMMON/SAVE/NP,INDEX,SRS(50),SCS(50)
1000 FORMAT(4I5)
1010 FORMAT(10F8.5)
1020 FORMAT(1H0,2BHINITIAL CONDITIONS - AT MOST,13,14H ITERATION(S) .
      * 18HWILL BE ATTEMPTFD.)
1030 FORMAT(1H0,19HUNIFORM ACCURACY OF,F8.5,16H PERCENT IS NOT ,
      * 47HATTAINED FOR SLIPSTREAM RADIUS AND CIRCULATION ,
      * 14HDISTRIBUTIONS.,/,BH AT MOST,13,19H MORE ITERATION(S) .
      * 18HWILL BE ATTEMPTED.)
1040 FORMAT(1H0,47HRESULTS OF THIS ITERATION INDICATE AN IMPROPER ,
      * 42HSTREAMLINE SHAPE - ITERATION IS TERMINATED)
1050 FORMAT(1H0,47HRESULTS OF THIS ITERATION INDICATE AN IMPROPER ,
      * 50HCIRCULATION DISTRIBUTION - ITERATION IS TERMINATED)
1060 FORMAT(1H0,19HUNIFORM ACCURACY OF,F8.5,12H PERCENT IS ,
      * 47HATTAINED FOR SLIPSTREAM RADIUS AND CIRCULATION ,
      * 14HDISTRIBUTIONS.)
1070 FORMAT(1H0,19HUNIFORM ACCURACY OF,F8.5,16H PERCENT IS NOT ,
      * 47HATTAINED FOR SLIPSTREAM RADIUS AND CIRCULATION ,
      * 14HDISTRIBUTIONS.)
1080 FORMAT(1H ,47HITERATION IS TERMINATED. DYNAMIC AND KINEMATIC ,
      * 41HCONDITIONS ON STREAMLINE WILL BE CHECKED.)
      READ 1000,IM,ID,IY
10 READ 1000,MM,NN,NITER           $ IF (MM) 190,190,20
20 READ 1010,CC,LAMBDA,ACC
      READ 1010,(XS(I),I=1,MM)
      NXG=MM                       $ NXG=NN
      ALPHA=1.8                    $ BETA=0.0
      DO 30 I=1,NXS
      B(I)=0.0                      $ FZ(I)=FJ(0.0,1)
30 CONTINUE
      DO 40 I=1,NXG
      A(I)=0.0
40 CONTINUE
      CALL SHAPE(2.0,0,0,TI)        $ FI=CC-(CC/(2.0*TI))**2
      GI=SQRTF(LAMBDA**2+FI)-LAMBDA
      ITER=0                        $ ACCP=100.0*ACC
      INDEX=1                       $ CALL OUTPUT
      M=NP+1                         $ SC(M)=SCS(M)=GI
      INDEX=2                        $ PRINT 1020,NITER
      DO 130 ITER=1,NITER
      TIS=TI                          $ N=NXS
      DO 50 I=1,N
      ZZ=XS(I)                        $ CALL TOPBOT(ZZ)
      CALL LIMITCHK                   $ CALL BEGNS(I)
50 CONTINUE
      CALL MATINV(RHS,N,LHS,1,DET)
      DO 60 J=1,N

```

```

        B(J)=LHS(J,1)
60  CONTINUE
    CALL SHAPE(2,0.0,TT)          $ FI=CC-(CC/(2.0*TI))**2
    GI=SQRTF(LAMBDA**2+FI)-LAMBDA $ N=NXG
    DO 70 I=1,N
        ZZ=XG(I)                  $ CALL TOPBOT(ZZ)
    CALL LIMITCHK                 $ CALL AEGNS(I)
70  CONTINUE
    CALL MATINV(RHS,N,LHS,1,DET)
    DO 80 J=1,N
        A(J)=LHS(J,1)
80  CONTINUE
    CALL OUTPUT
    CALL SHAPE(1,0.05,TTEST)      $ IF (TTEST-1.0) 90,140,140
90  CALL VORTEX(0.01,GI,GTEST)   $ IF (GTEST-GI) 150,150,100
100 SR(M)=TI                     $ SRS(M)=TIS
    DO 102 I=2,M
        CACC=ACC*SC(I)           $ TACC=ACC*SR(I)
        IF (ABSF(SC(I))-SCS(I))-CACC) 101,101,110
101 IF (ABSF(SR(I))-SRS(I))-TACC) 102,102,110
102 CONTINUE
    GO TO 160
110 LEFT=NITER-ITER              $ IF (LEFT) 170,170,120
120 PRINT 1030,ACCP,LEFT
130 CONTINUE
140 PRINT 1040                    $ GO TO 10
150 PRINT 1050                    $ GO TO 10
160 PRINT 1060,ACCP              $ GO TO 180
170 PRINT 1070,ACCP              $ GO TO 180
180 PRINT 1080                    $ CALL DYKICHCK
    GO TO 10
190 FND

```

```

SUBROUTINE AEGNS(I)
EXTERNAL GJ
TYPE REAL LHS,LAMBDA
COMMON/INPUT/LAMBDA,CC,ALPHA,BETA
COMMON/INTGND/NGEES,TT,ZZ,N,K,GI
COMMON/LIMITS/TOP(7),BOT(7),NGD(7)
COMMON/MATRIX/RHS(50,50),LHS(50,1)
DIMENSION XI(400),GTTR(400)
DIMENSION R(5),U(5)
DATA (R=0.1477621124,0.1346333597,0.1095431813,0.07472567458,
*      0.03333567215),
*      (U=0.0744371695,0.2166976971,0.3397047841,0.4325316833,
*      0.4869532643)
    CALL SHAPE(1,ZZ,TT)          $ CALL FACTOR(ZZ,FAC)
    CALL VORTEX(ZZ,GI,GAM)      $ CON=2.0*GAM**2*FAC
    FF=CC-(CC/(2.0*TT))**2
    NN = N+1
    KK = 0
    DO 70 J=1,7
        IF (ABSF(TOP(J))-BOT(J))-0.0000001)70,70,10
10  NTIME = NGD(J)
    R = TOP(J)  $ A = BOT(J)
    DO 60 II=1,NTIME
        XL = A+(II-1)*(B-A)/NTIME  $ XU = B-(NTIME-II)*(B-A)/NTIME
        D = XU-XL  $ S = (XU+XL)/2.0
    DO 50 L=1,10

```

```

      KK = KK+1
      IF(L-5)20,20,30
20  JJ = L      $      XI(KK) = S+D*U(JJ)
      GO TO 40
30  JJ = 11-L  $      XI(KK) = S-D*U(JJ)
40  CALL SHAPE(1,XI(KK),T)
      CALL FACTOR(XI(KK),ROOT)
      CALL GEES(1,TT,T,ZZ,XI(KK),G,GT,GTT)
      GTTR(KK) = D*R(JJ)*GTT*ROOT
50  CONTINUE
60  CONTINUE
70  CONTINUE
      DO 140 J=1,NN
      K = J      $      IF(J-NN)80,90,90
80  RHS(I,J)=FF*TT*GJ(ZZ,J)/CON      $ GO TO 100
90  RHS(I,J)=TT*(LAMBDA+FF*GI/CON-FF/(FAC*GAM))/GI
100 DO 130 L=1,KK
      IF(J-NN)110,120,120
110 RHS(I,J) = RHS(I,J)+GTTR(L)*GJ(XI(L),J)
      GO TO 130
120 RHS(I,J) = RHS(I,J)+GTTR(L)
130 CONTINUE
140 CONTINUE
      LHS(I,1)=-RHS(I,NN)
      END

```

```

SUBROUTINE RFONS(I)
EXTERNAL BINT,FJ
TYPE REAL LHS,LAMBDA
COMMON/ADDED/FZ(50),TI
COMMON/INPUT/LAMBDA,CC,ALPHA,BETA
COMMON/INTGND/NGEES,TT,ZZ,N,K,GI
COMMON/MATRIX/RHS(50,50),LHS(50,1)
NN=N+1      $ CALL SHAPE(1,ZZ,TT)
GTTG=GGM=0.0
NGEES=1      $ CALL ONEINTGL(BINT,GTTG)
NGEES=3      $ CALL ONEINTGL(BINT,GGM)
ADD=GGM+ALPHA*(TT-1.0)*GTTG
DO 30 J=1,NN
K=J      $ IF (J-NN) 10,20,20
10 CON=FJ(ZZ,J)-FZ(J)
RHS(I,J)=LAMBDA*TT*CON+(LAMBDA+GI)*TI*FZ(J)+ALPHA*CON*GTTG
GO TO 30
20 RHS(I,J)=(LAMBDA+GI)*TI*(1.0-0.5*TI)-LAMBDA*TT*(1.0-0.5*TT)+ADD
30 CONTINUE
LHS(I,1)=RHS(I,NN)
END

```

```

FUNCTION BINT(Z)
EXTERNAL FJ
COMMON/ADDED/FZ(50),TI
COMMON/INPUT/LAMBDA,CC,ALPHA,BETA
COMMON/INTGND/NGEES,TT,ZZ,N,K,GI
CALL SHAPE(1,Z,T)      $ CALL VORTEX(Z,GI,GAM)
CALL FACTOR(Z,FAC)      $ GAM=FAC*GAM
CALL GEES(NGEES,TT,T,ZZ,Z,G,GT,GTT)
GO TO (10,30,20),NGEES
10 BINT=GTT*GAM      $ GO TO 30
20 BINT=-G*GAM
30 END

```



```

SUBROUTINE DYKICHCK
EXTERNAL GTG,GGG
TYPE REAL LAMBDA
COMMON/INPUT/LAMBDA,CC,ALPHA,BETA
COMMON/INTGND/NGEES,TT,ZZ,N,K,G1
COMMON/NUMBERXS/NXS,NXG
COMMON/PRINT/XS(50),XG(50),XP(50),SR(50),SC(50),ITER,IM,ID,IY
DIMENSION X(19)
DATA (X=0.01,0.02,0.03,0.04,0.05,0.10,0.15,0.20,0.30,0.40,0.50,
*      0.75,1.00,1.25,1.50,2.00,3.00,5.00,10.00)
1000 FORMAT(1H1,22X,40H R O T O R O U T O F G R O U N D ,
*          35H E F F E C T ( N A S 1 - 6 3 4 9 ),5X,1H(.I2,1H/,I2,
*          1H/,I2,1H))
1010 FORMAT(1H0,35X,29HDAMPING COEFFICIENTS, ALPHA =,F5.2,9H , BETA =,
*          F5.2,/,36X,
*          24HLOADING COEFFICIENT, C =,F7.4,/,36X,
*          23HADVANCE RATIO, LAMBDA =,F7.4,/,36X,
*          36HNO. OF SHAPE COLLOCATION POINTS, M =,I3,/,36X,
*          36HNO. OF GAMMA COLLOCATION POINTS, N =,I3,/,36X,
*          16HHUB RADIUS = 0.0)
1020 FORMAT(1H0,/,45H NUMERICAL CHECK OF DYNAMIC (FORCE-FREE) AND ,
*          47HKINEMATIC (STREAMLINE) CONDITIONS ON SLIPSTREAM,/)
1030 FORMAT(1H ,50X,8HDYNAMIC,25X,10HKINEMATIC,/,54X,
*          20HU*GAMMA SHOULD EQUAL,11X,19HTOTAL (CAP) PSI ON ,
*          10HSLIPSTREAM,/,9X,36HTOTAL X-VEL. SLIPSTREAM VORTICITY,
*          18X,3HF/2,15X,36HSHOULD EQUAL ITS VALUE AT X=INFINITY,
*          /,8X,36HON SLIPSTREAM, PER UNIT X-LENGTH,9X,8H-----,
*          14H-----,5X,31H-----,
*          7H-----,/,4H X,9X,4HU(X),14X,8HGAMMA(X),17X,3HLHS,11X,
*          3HRHS,17X,3HLHS,13X,3HRHS,/)
1040 FORMAT(1H ,F5.2,F12.5,F20.5,F22.5,F14.5,F20.5,F16.5)
1050 FORMAT(1H ,5H INF.,F12.5,F20.5,F22.5,F14.5,F20.5,F16.5)
PRINT 1000,IM,ID,IY
PRINT 1010,ALPHA,BETA,CC,LAMBDA,NXS,NXG
PRINT 1020 $ PRINT 1030
CALL SHAPE(2.0,0,TT) $ CB=0.5*TI**2*(LAMBDA+G1)
DO 60 I=1,20
IF (I-20) 20,10,10
10 U=LAMBDA+0.5*G1 $ GAM=G1
CA=0.5*(CC-(CC/(2.0*TI))**2) $ GO TO 30
PSI=CB $ CALL SHAPE(1,ZZ,TT)
20 ZZ=X(I) $ CALL FACTOR(ZZ,FAC)
CA=0.5*(CC-(CC/(2.0*TT))**2) $ CALL TOPBOT(ZZ)
CALL VORTEX(ZZ,G1,GAM) $ U=LAMBDA
GAM=FAC*GAM $ CALL TWOINTGL(GTG,GGG,U,PSI)
CALL LIMITCHK $ IF (I-20) 40,50,50
PSI=0.5*LAMBDA*TT**2
30 UG=U*GAM
40 PRINT 1040,ZZ,U,GAM,UG,CA,PSI,CB
GO TO 60
50 PRINT 1050,U,GAM,UG,CA,PSI,CB
60 CONTINUE
END

```

```

SUBROUTINE FACTOR(X,FAC)
EXTERNAL FPJ
COMMON/COEFS/A(50),B(50)
COMMON/NUMBERXS/NXS,NXG
TP=0.0
DO 10 I=1,NXS
TP=TP+B(I)*FPJ(X,I)
10 CONTINUE
FAC=SQRTF(1.0+TP**2)
END

```

```

FUNCTION FJ(X,J)
FJ=EXPF(-J*X)
END

```

```

FUNCTION FPJ(X,J)
FPJ=-J*EXPF(-J*X)
END

```

```

SUBROUTINE GEES(NUM,TT,T,ZZ,Z,G,GT,GTT)
PI=3.1415927                $ TERM=SQRTF(TT*T)
DEL=(ZZ-Z)**2              $ ATOP=DEL+TT**2-T**2
BTOP=DEL+T**2-TT**2        $ ABOT=8.0*PI*TERM*T
BBOT=8.0*PI*TERM*TT
A=ATOP/ABOT                $ R=BTOP/BBOT
ARG=1.0+((TT-T)**2+(ZZ-Z)**2)/(2.0*TT*T)
CALL QPMHALF(ARG,QPH,QMH)  $ GO TO (30,20,10),NUM
10 G=TERM*QPH/(2.0*PI)
20 GT=(B*QPH+A*QMH)/(ARG**2-1.0)
30 GTT=(A*QPH+B*QMH)/(ARG**2-1.0)
END

```

```

FUNCTION GGG(Z)
COMMON/INTGND/NGEES,TT,ZZ,N,K,GI
CALL SHAPE(1,Z,T)          $ CALL VORTEX(Z,GI,G)
CALL FACTOR(Z,FAC)         $ G=FAC*G
CALL GEES(3,TT,T,ZZ,Z,GG,DUM,DUMM)
GGG=GG*G
END

```

```

FUNCTION GJ(X,J)
IF (J-1) 10,10,20
10 GJ=EXPF(-3.0*X)/SQRTF(X)    $ GO TO 30
20 GJ=X**(-0.84+0.51*J)*EXPF(-3.0*X)
30 END

```

```

FUNCTION GTG(Z)
COMMON/INTGND/NGEES,TT,ZZ,N,K,GI
CALL SHAPE(1,Z,T)          $ CALL VORTEX(Z,GI,G)
CALL FACTOR(Z,FAC)         $ G=FAC*G
CALL GFES(1,TT,T,ZZ,Z,DUM,DUMM,GTT)
GTG=GTT*G/TT
END

```

```

SUBROUTINE LIMITCHK
COMMON/LIMITS/TOP(7),BOT(7),NGD(7)
DO 40 I=1,7
IF (BOT(I)-TOP(I)) 40,40,10
10 IF (I-7) 20,30,30
20 BOT(I+1)=BOT(I)
30 ROT(I)=TOP(I)
40 CONTINUE
END

```

```

SUBROUTINE MATINV(A,N,B,M,DETERM)
DIMENSION IPIVOT(50),A(50,50),B(50,1),INDEX(50,2),PIVOT(50)
DETERM=1.0
DO 10 J=1,N
IPIVOT(J)=0
10 CONTINUE
DO 200 I=1,N
AMAX=0.0
DO 60 J=1,N
IF (IPIVOT(J)-1) 20,60,20
20 DO 50 K=1,N
IF (IPIVOT(K)-1) 30,50,240
30 IF (ABSF(AMAX)-ABSF(A(J,K))) 40,50,50
40 IROW=J $ ICOLUM=K
AMAX=A(J,K)
50 CONTINUE
60 CONTINUE
IPIVOT(ICOLUM)=IPIVOT(ICOLUM)+1 $ IF (IROW-ICOLUM) 70,110,70
70 DETERM=-DETERM
DO 80 L=1,N
SWAP=A(IROW,L) $ A(IROW,L)=A(ICOLUM,L)
A(ICOLUM,L)=SWAP
80 CONTINUE
IF (M) 110,110,90
90 DO 100 L=1,M
SWAP=B(IROW,L) $ B(IROW,L)=B(ICOLUM,L)
B(ICOLUM,L)=SWAP
100 CONTINUE
110 INDEX(I,1)=IROW
INDEX(I,2)=ICOLUM $ PIVOT(I)=A(ICOLUM,ICOLUM)
DETERM=DETERM*PIVOT(I) $ A(ICOLUM,ICOLUM)=1.0
DO 120 L=1,N
A(ICOLUM,L)=A(ICOLUM,L)/PIVOT(I)
120 CONTINUE
IF (M) 150,150,130
130 DO 140 L=1,M
B(ICOLUM,L)=B(ICOLUM,L)/PIVOT(I)
140 CONTINUE
DO 200 L1=1,N
IF(L1-ICOLUM) 160,200,160
160 T=A(L1,ICOLUM) $ A(L1,ICOLUM)=0.0
DO 170 L=1,N
A(L1,L)=A(L1,L)-A(ICOLUM,L)*T
170 CONTINUE
IF (M) 200,200,180
180 DO 190 L=1,M
B(L1,L)=B(L1,L)-B(ICOLUM,L)*T
190 CONTINUE
200 CONTINUE
DO 230 I=1,N
L=N+1-I
IF (INDEX(L,1)-INDEX(L,2)) 210,230,210
210 JROW=INDEX(L,1) $ JCOLUM=INDEX(L,2)
DO 220 K=1,N
SWAP=A(K,JROW) $ A(K,JROW)=A(K,JCOLUM)
A(K,JCOLUM)=SWAP
220 CONTINUE
230 CONTINUE
240 RETURN
END

```

```

SUBROUTINE NGAUSS(B,A,FX,NTIME,INTEGRAL)
TYPE REAL INTEGRAL
DIMENSION R(5),U(5)
DATA (R=0.1477621124,0.1346333597,0.1095431813,0.07472567458,
*      0.03333567215),
*      (U=0.0744371695,0.2166976971,0.3397047841,0.4325316833,
*      0.4869532643)
INTEGRAL=0.0
DO 20 J=1,NTIME
XL=A+(J-1)*(B-A)/NTIME          $ XU=B-(NTIME-J)*(B-A)/NTIME
D=XU-XL                          $ S=(XU+XL)/2.0
TEMP=0.0
DO 10 K=1,5
TEMP=TEMP+R(K)*(FX(S+D*U(K))+FX(S-D*U(K)))
10 CONTINUE
TEMP=TEMP*D                      $ INTEGRAL=INTEGRAL+TEMP
20 CONTINUE
END

```

```

SUBROUTINE ONEINTGL(FA,A)
COMMON/LIMITS/TOP(7),BOT(7),NGD(7)
DO 20 I=1,7
IF (ABS(TOP(I)-BOT(I))-0.0000001) 20,20,10
10 CALL NGAUSS(TOP(I),BOT(I),FA,NGD(I),AA)
A=A+AA
20 CONTINUE
END

```

```

SUBROUTINE OUTPUT
TYPE REAL LAMBDA
COMMON/ADDED/FZ(50),TI
COMMON/COEFS/A(50),B(50)
COMMON/INPUT/LAMBDA,CC,ALPHA,BETA
COMMON/INTGND/NGEES,TT,ZZ,N,K,G1
COMMON/NUMBERXS/NXS,NXG
COMMON/PRINT/XS(50),XG(50),XP(50),SR(50),SC(50),ITER,IM,ID,IY
COMMON/SAVE/NP,INDEX,SRS(50),SCS(50)
1000 FORMAT(1H1,22X,40H O T O R O U T O F G R O U N D ,
*      35H E F F E C T ( N A S 1 - 6 3 4 9 ),5X,1H(,12,1H/,12,
*      1H/,12,1H))
1010 FORMAT(1H0,35X,29HDAMPING COEFFICIENTS, ALPHA =,F5.2,9H , BETA =,
*      F5.2,/,36X,
*      24HLOADING COEFFICIENT, C =,F7.4,/,36X,
*      23HADVANCE RATIO, LAMBDA =,F7.4,/,36X,
*      16HHUB RADIUS = 0.0)
1020 FORMAT(1H0,21X,29HSHAPE COLLOCATION POINTS, M =,I3,12X,
*      29HGAMMA COLLOCATION POINTS, N =,I3,/)
1030 FORMAT(1H ,28X,5HX SUB,I3,2H =,F8.4,26X,5HX SUB,I3,2H =,F8.4)
1040 FORMAT(1H ,72X,5HX SUB,I3,2H =,F8.4)
1050 FORMAT(1H ,28X,5HX SUB,I3,2H =,F8.4)
1060 FORMAT(1H0,13HITERATION NO.,I3,/)
1070 FORMAT(1H ,79X,35HSLIPSTREAM SLIPSTREAM CIRCULATION,/,7X,
*      18HSHAPE COEFFICIENTS,14X,18HGAMMA COEFFICIENTS,11X,1HX,
*      11X,30HRADIUS, T GAMMA SUB S,/)
1071 FORMAT(1H ,4X,10HB SUB 1 =,F12.4,10X,10HA SUB 1 =,F12.4,8X,
*      4H,000,11X,6H1.0000,F18.4)
1072 FORMAT(1H ,4X,10HB SUB 1 =,F12.4,10X,10HA SUB 1 =,F12.4,8X,
*      4H,000,11X,6H1.0000,10X,8HINFINITY)
1080 FORMAT(1H ,4X,5HB SUB,I3,2H =,F12.4,10X,5HA SUB,I3,2H =,F12.4,
*      F12.3,F17.4,F18.4)
1090 FORMAT(1H ,4X,5HB SUB,I3,2H =,F12.4,10X,5HA SUB,I3,2H =,F12.4,5X,
*      8HINFINITY,F16.4,F18.4)

```

```

1100 FORMAT(1H ,4X,5HB SUB,I3,2H =,F12.4,10X,5HA SUB,I3,2H =,F12.4)
1110 FORMAT(1H ,4X,5HB SUB,I3,2H =,F12.4,32X,F12.3,F17.4,F18.4)
1120 FORMAT(1H ,4X,5HB SUB,I3,2H =,F12.4,37X,8HINFINITY,F16.4,F18.4)
1130 FORMAT(1H ,4X,5HR SUB,I3,2H =,F12.4)
1140 FORMAT(1H ,36X,5HA SUB,I3,2H =,F12.4,F12.3,F17.4,F18.4)
1150 FORMAT(1H ,36X,5HA SUB,I3,2H =,F12.4,5X,8HINFINITY,F16.4,F18.4)
1160 FORMAT(1H ,36X,5HA SUB,I3,2H =,F12.4)
1170 FORMAT(1H ,58X,F12.3,F17.4,F18.4)
1180 FORMAT(1H ,63X,8HINFINITY,F16.4,F18.4)
      NP=30
      DO 60 I=2,NP
      GO TO (5,4),INDEX
      4  SRS(I)=SR(I)          $ SC5(I)=SC(I)
      GO TO 55
      5  IF (I-5) 30,30,10
      10 IF (I-10) 40,40,20
      20 IF (I-17) 45,45,25
      25 IF (I-25) 50,50,51
      30 J=2*I-3              $ XP(I)=0.01*J
      GO TO 55
      40 J=I-4               $ XP(I)=0.05*J
      GO TO 55
      45 J=I-7               $ XP(I)=0.10*J
      GO TO 55
      50 J=I-13              $ XP(I)=0.25*J
      GO TO 55
      51 J=I-22              $ XP(I)=1.00*J
      55 CALL SHAPE(I,XP(I),SR(I)) $ CALL VORTEX(XP(I),GI,SC(I))
      60 CONTINUE
      65 PRINT 1000,IM,JD,IY          $ PRINT 1010,ALPHA,BETA,CC,LAMBDA
      PRINT 1020,NXS,NXG              $ IF (NXS-NXG) 70,70,80
      70 M=NXS                          $ GO TO 90
      80 M=NXG
      90 PRINT 1030,(I,XS(I),I,XG(I),I=1,M)
      M=M+1                            $ IF (NXS-NXG) 100,120,110
      100 PRINT 1040,(I,XG(I),I=M,NXG) $ GO TO 120
      110 PRINT 1050,(I,XS(I),I=M,NXS)
      120 PRINT 1060,ITER              $ PRINT 1070
      IF (NXS-NXG) 130,140,140
      130 IF (NXG-NP) 150,150,160
      140 IF (NXS-NP) 150,150,170
      150 M=NP+1                       $ GO TO 180
      160 M=NXG                         $ GO TO 180
      170 M=NXS
      180 KOUNT=1                       $ IF (ITER) 181,181,182
      181 PRINT 1071,B(I),A(I),GI      $ GO TO 183
      182 PRINT 1072,B(I),A(I)
      183 DO 390 I=2,M
      IF (I-NXS) 190,190,220
      190 IF (I-NXG) 200,200,210
      200 IF (I-NP) 250,250,260
      210 IF (I-NP) 290,290,300
      220 IF (I-NXG) 230,230,240
      230 IF (I-NP) 330,330,340
      240 IF (I-NP) 370,370,380
      250 PRINT 1080,I,B(I),I,A(I),XP(I),SR(I),SC(I)
      GO TO 390
      260 GO TO (270,280),KOUNT
      270 PRINT 1090,I,B(I),I,A(I),TI,GI
      KOUNT=2                          $ GO TO 390
      280 PRINT 1100,I,B(I),I,A(I)     $ GO TO 390
      290 PRINT 1110,I,B(I),XP(I),SR(I),SC(I)
      GO TO 390
      300 GO TO (310,320),KOUNT
      310 PRINT 1120,I,B(I),TI,GI     $ GO TO 390
      KOUNT=2

```

```

320 PRINT 1130,I,B(I)          $ GO TO 390
330 PRINT 1140,I,A(I),XP(I),SR(I),SC(I)
    GO TO 390
340 GO TO (350,360),KOUNT
350 PRINT 1150,I,A(I),TI,GI
    KOUNT=2                    $ GO TO 390
360 PRINT 1160,I,A(I)          $ GO TO 390
370 PRINT 1170,XP(I),SR(I),SC(I) $ GO TO 390
380 PRINT 1180,TI,GI
390 CONTINUE
    END

```

```

SUBROUTINE QPMHALF(Z,OPH,QMH)
TYPE RFAL KPRIMESQ,K
KPRIMESQ=1.0-(2.0/(Z+1.0))    $ A1=KPRIMESQ
A2=A1*A1                      $ A3=A2*A1
A4=A2*A2                      $ ALO=LOGF(1.0/KPRIMESQ)
K=SQRTF(2.0/(Z+1.0))        $ B=SQRTF(2.0*(Z+1.0))
ELE=1.00000000000+.44325141463*A1+.06260601220*A2
*      +.04757383546*A3+.01736506451*A4+
*      (.24998368310*A1+.09200180037*A2+
*      .04069697526*A3+.00526449639*A4)*ALO
ELK=1.38629436112+.09666344259*A1+.03590092383*A2
*      +.03742563713*A3+.01451196212*A4+
*      (.50000000000+.12498593597*A1+.06880248576*A2
*      +.03328355346*A3+.00441787012*A4)*ALO
OPH=Z*K*ELK-B*ELE            $ QMH=K*ELK
END

```

```

SUBROUTINE SHAPE(KODF,X,S)
EXTERNAL FJ
COMMON/ADDFD/FZ(50),TI
COMMON/COEFS/A(50),B(50)
COMMON/NUMBERXS/NXS,NXG
GO TO (10,30),KODF
10 S=TI
    DO 20 J=1,NXS
    S=S+B(J)*FJ(X,J)
20 CONTINUE
    GO TO 50
30 S=1.0
    DO 40 J=1,NXS
    S=S-R(J)*FZ(J)
40 CONTINUE
50 END

```

```

SUBROUTINE TOPROT(ZZ)
COMMON/LIMITS/TOP(7),BOT(7),NGD(7)
DO 10 I=1,7
TOP(I)=BOT(I)+0.0            $ NGD(I)=1
10 CONTINUE
    NGD(4)=3
    IF (ABSF(ZZ)-0.0000001) 80,80,20
20 IF (ZZ) 70,80,30
30 IF (ABSF(ZZ-0.2)-0.0000001) 100,100,40
40 IF (ZZ-0.2) 100,100,50
50 IF (ABSF(ZZ-3.0)-0.0000001) 140,140,60
60 IF (ZZ-3.0) 140,140,150
70 NGD(4)=2                    $ FPS=0.1
    GO TO 90
80 FPS=0.05

```

```

90 TOP(4)=BOT(5)=EPS          $ TOP(5)=BOT(6)=1.0
   TOP(6)=BOT(7)=10.0        $ TOP(7)=100.0
   GO TO 180
100 IF (ZZ-0.05) 110,110,120
110 EPS=ZZ                    $ GO TO 130
120 EPS=0.05
130 TOP(3)=BOT(4)=ZZ-EPS     $ TOP(4)=BOT(5)=ZZ+EPS
   GO TO 170
140 TOP(2)=BOT(3)=0.15       $ TOP(3)=BOT(4)=ZZ-0.05
   GO TO 160
150 TOP(1)=BOT(2)=0.15       $ TOP(2)=BOT(3)=ZZ-1.0
   TOP(3)=BOT(4)=ZZ-0.05
160 TOP(4)=BOT(5)=ZZ+0.05
170 TOP(5)=BOT(6)=ZZ+1.0     $ TOP(6)=BOT(7)=ZZ+10.0
   TOP(7)=ZZ+100.0
180 END

```

```

SUBROUTINE TWOINTGL(FA,FB,A,B)
COMMON/LIMITS/TOP(7),BOT(7),NGD(7)
DO 20 I=1,7
IF (ABSF(TOP(I)-BOT(I))-0.0000001) 20,20,10
10 CALL NGAUSS(TOP(I),BOT(I),FA,NGD(I),AA)
   CALL NGAUSS(TOP(I),BOT(I),FB,NGD(I),BB)
   A=A+AA          $ B=B+BB
20 CONTINUE
END

```

```

SUBROUTINE VORTEX(X,GI,V)
EXTERNAL GJ
COMMON/COEFS/A(50),B(50)
COMMON/NUMBERXS/NXS,NXG
V=1.0
DO 10 J=1,NXG
V=V+A(J)*GJ(X,J)
10 CONTINUE
V=GI*V
END
      END      ROTORGE
      FINIS

```

FIRST CLASS MAIL

POSTMASTER: If Undeliverable (Section 15
Postal Manual) Do Not Return

"The aeronautical and space activities of the United States shall be conducted so as to contribute . . . to the expansion of human knowledge of phenomena in the atmosphere and space. The Administration shall provide for the widest practicable and appropriate dissemination of information concerning its activities and the results thereof."

— NATIONAL AERONAUTICS AND SPACE ACT OF 1958

NASA SCIENTIFIC AND TECHNICAL PUBLICATIONS

TECHNICAL REPORTS: Scientific and technical information considered important, complete, and a lasting contribution to existing knowledge.

TECHNICAL NOTES: Information less broad in scope but nevertheless of importance as a contribution to existing knowledge.

TECHNICAL MEMORANDUMS: Information receiving limited distribution because of preliminary data, security classification, or other reasons.

CONTRACTOR REPORTS: Scientific and technical information generated under a NASA contract or grant and considered an important contribution to existing knowledge.

TECHNICAL TRANSLATIONS: Information published in a foreign language considered to merit NASA distribution in English.

SPECIAL PUBLICATIONS: Information derived from or of value to NASA activities. Publications include conference proceedings, monographs, data compilations, handbooks, sourcebooks, and special bibliographies.

TECHNOLOGY UTILIZATION PUBLICATIONS: Information on technology used by NASA that may be of particular interest in commercial and other non-aerospace applications. Publications include Tech Briefs, Technology Utilization Reports and Notes, and Technology Surveys.

Details on the availability of these publications may be obtained from:

SCIENTIFIC AND TECHNICAL INFORMATION DIVISION
NATIONAL AERONAUTICS AND SPACE ADMINISTRATION
Washington, D.C. 20546